



**BRNO UNIVERSITY OF TECHNOLOGY**

VYSOKÉ UČENÍ TECHNICKÉ V BRNĚ

**FACULTY OF CHEMISTRY**

FAKULTA CHEMICKÁ

**INSTITUTE OF MATERIALS SCIENCE**

ÚSTAV CHEMIE MATERIÁLŮ

**MORPHOGENESIS AND VISCOELASTIC PROPERTIES OF  
DIMETHACRYLATE NETWORKS**

MORFOGENEZE A VISKOELASTICKÉ VLASTNOSTI DIMETHAKRYLÁTOVÝCH SÍTÍ

**DOCTORAL THESIS**

DIZERTAČNÍ PRÁCE

**AUTHOR**

AUTOR PRÁCE

Ing. Zdeněk Bystřický

**SUPERVISOR**

ŠKOLITEL

prof. RNDr. Josef Jančář, CSc.

**BRNO 2019**

## ABSTRACT

The thesis deals with the investigation of dimethacrylate networks morphogenesis. Simple model resin mixtures used in this work were based on the monomers, which are typically employed as the components of matrix systems of dental resin composites. Kinetics and mechanisms of polymer networks formation were studied with respect to a structure of monomers, molar ratio of comonomers, and a concentration of the radical polymerization initiation system. Calculated profiles of functional groups conversion and polymerization rate were used as a basis for understanding and interpretation of mechanisms of networks morphogenesis and comparison with known models. Furthermore, kinetics of thermal degradation process was studied because it is closely related to the morphology of the networks. Then, temperature dependence of viscoelastic modulus was determined and the relationship between supramolecular structure of dimethacrylate networks and their viscoelastic response within the given temperature range was quantified.

Polymerization kinetics was studied by differential photo-calorimetry (DPC) and infrared spectroscopy (FTIR). Process of thermal degradation was analyzed using thermo-gravimetric analysis (TGA). Viscoelastic parameters were measured using dynamic-mechanical analysis (DMA).

Reactivity of dimethacrylate systems is derived from the molecular structure of monomers, because it affects mobility of reacting species during polymerization. Kinetics of polymerization is controlled by diffusion. Rate of diffusion is given by the monomer rigidity, concentration of functional groups, and an impact of physical interactions. The mobility restrictions, affecting growing chains, pendant side chains and free monomers, lead to monomolecular termination of macroradicals and limited degree of conversion. Since the mobility is restricted severely from the early phases of the reaction, i.e. from the gel point, phase separation is suppressed despite any potential thermodynamic instability, and the copolymerization process is random. This was confirmed by identification of single glass transition temperature in DMA experiments of copolymers. Heterogeneous character of morphogenesis is related to a varying reactivity of pendant functional groups. In the early phases of the polymerization, propagation proceeds via intramolecular attack of the radical site to the pendant, leading to the primary cycle formation. Probability of the cyclization is increased by flexibility of the monomer backbone. Heterogeneity of the curing reaction is characterized by formation of internally crosslinked structures, i.e. microgels, followed by their interconnections. On contrary, rigidity of the monomer leads to a higher effectivity of crosslinking and more homogeneous morphology of the corresponding networks. Presence of the inhomogeneities, characterized by coexistence of structurally distinct regions, is related to a two-step mechanism of thermal decomposition. Progress of the storage modulus and the glass transition temperature correlate with the network stiffness, effectivity of crosslinking, and the presence of physical interactions that reinforce the structure beyond the scope of covalent crosslinking. Structural heterogeneity is manifested by broad transition region indicating wide variations in relaxation times. Experimental data are in qualitative correlation with the numerical models that simulates kinetics of free radical network polymerization.

## **KEYWORDS**

Dimethacrylate monomers, radical polymerization, copolymerization, polymerization kinetics, multifunctional polymer networks, morphogenesis, viscoelasticity, thermal degradation

# TABLE OF CONTENTS

<b>1</b>	<b>INTRODUCTION .....</b>	<b>5</b>
<b>2</b>	<b>CURRENT STATE OF RESEARCH TOPIC.....</b>	<b>6</b>
2.1.1	Comonomer formulations.....	6
<b>2.2</b>	<b>Monomer structure and associated properties .....</b>	<b>7</b>
2.2.1	Viscosity.....	7
2.2.2	Reactivity.....	8
<b>2.3</b>	<b>Radical polymerization of multifunctional monomers.....</b>	<b>8</b>
2.3.1	Aspects of the polymerization of multifunctional monomers.....	9
2.3.2	Photo-polymerization.....	10
2.3.3	Photo-polymerization kinetics .....	11
<b>2.4</b>	<b>Special features of multifunctional network formation.....</b>	<b>13</b>
<b>3</b>	<b>AIM OF THE THESES.....</b>	<b>15</b>
<b>4</b>	<b>EXPERIMENTAL PART .....</b>	<b>16</b>
<b>4.1</b>	<b>Materials.....</b>	<b>16</b>
<b>4.2</b>	<b>Experiments overview .....</b>	<b>17</b>
4.2.1	Photo-polymerization kinetics (DPC) .....	17
4.2.2	Determination of degree of double bonds conversion (FTIR).....	18
4.2.3	Kinetics of thermal degradation (TGA) .....	18
4.2.4	Viscoelasticity of the networks (DMA) .....	19
<b>5</b>	<b>Results and Discussion.....</b>	<b>21</b>
<b>5.1</b>	<b>Morphogenesis of dimethacrylate network .....</b>	<b>21</b>
5.1.1	Effects of monomer structure .....	21
5.1.2	Effects of comonomers ratio.....	28
<b>5.2</b>	<b>Viscoelastic behavior of dimethacrylate networks .....</b>	<b>36</b>
5.2.1	Homopolymers.....	37
5.2.2	Copolymers.....	40
<b>6</b>	<b>CONCLUSION .....</b>	<b>44</b>
<b>7</b>	<b>REFERENCES .....</b>	<b>46</b>
	<b>LIST OF FIGURES.....</b>	<b>52</b>
	<b>LIST OF TABLES .....</b>	<b>53</b>
	<b>LIST OF ABBREVIATIONS .....</b>	<b>54</b>
	Chemicals.....	54
	Experimental methods, others.....	54
	Equations .....	55
	<b>AUTHOR'S CV .....</b>	<b>56</b>

# 1 INTRODUCTION

Polymerization of multifunctional monomers leads to the formation of rigid, highly crosslinked networks that have found their use in a variety of applications including dental restoratives, microelectronics, optical lenses, UV-VIS curable adhesives and others. The application area of dimethacrylate monomers is related primarily to the field of restorative dentistry. This began in the mid 1960's with the introduction of suitable monomer species thanks to the pioneer research of Rafael L. Bowen [1,2]. Since then, dimethacrylate monomers-based restoratives have undergone significant development considering filler technology and mechanisms of initiation, whereas the monomer formulations have remained essentially unchanged [3,4].

The systematic studies, including evaluation of conversion, crosslinking, and network structure along with associated physical properties, are required for the optimization of desirable properties for development of durable materials. In order to attain desirable clinical outcomes of dimethacrylate based restoratives, most of the current research efforts are associated with the polymerization shrinkage phenomenon and incomplete curing reaction. First of these drawbacks is primarily related to the stress transmission to the adhesive bond and the remaining tooth structure resulting in the marginal crack formation, post-operative sensitivity, and the origination of secondary caries. The relatively moderate degree of double bonds conversion (typically ranging from 50 to 80 %) may be of concern for both the mechanical performance and the possible toxic effects or tissue irritation by untreated, leaching out low-molecular components [4–9]. Due to the complexity associated with the self-limitation of the process of multifunctional network formation, it is a challenging task to shed light on the mechanisms of the polymerization, determine the morphology of cured systems, and localize remaining unreacted double bonds. In the beginning, it is necessary to employ simple model resin mixtures before more complex formulations are taken into consideration. Commercial dental composites include complicated monomer systems with various additives influencing kinetics of polymer network formation. Moreover, presence of solid filler particles of large specific surface area can alter resin cure significantly by radical immobilization and de-activation [9,10].

This dissertation deals with the investigation of the copolymerization kinetics along with the dimethacrylate networks morphogenesis beginning from the structurally distinct simple monomer formulations, continuing with more comprehensive mixtures. The relationship between the morphology, kinetics of thermal degradation and viscoelastic properties will be investigated as well. Through a better understanding of the polymer network formation and property development with respect to the resulting morphology, the ultimate goal of achieving polymers with enhanced clinical outcomes is facilitated.

The following text is a shortened version of original thesis. It is limited to a brief introduction of the research topic and a presentation of the main results of the work.

## 2 CURRENT STATE OF RESEARCH TOPIC

As already mentioned above, modern era of dental acrylic materials is associated with the research of American dentist R. L. Bowen, who synthesized a new monomer, designed specifically for the purposes of restorative dentistry [1,2], i.e. 2,2-bis[4-(2-hydroxy-3-methacryloxyprop-1-oxy)-phenyl]-propane (Bis-GMA, Figure 1). This monomer is superior to methyl methacrylate because of its large molecular size and bulky chemical structure, providing lower volatility, lower polymerization shrinkage, more rapid hardening, and production of stronger and stiffer resins [3].

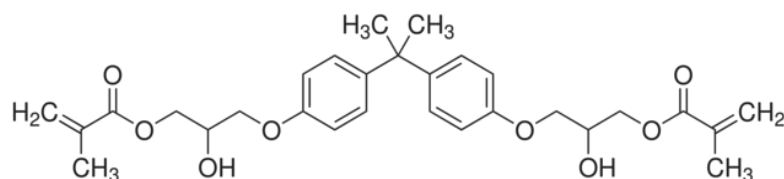


Figure 1: Bis-GMA (Bowen monomer).

### 2.1.1 Comonomer formulations

Predominantly used monomer in polymeric matrix formulations, often referred to as a base monomer, is already introduced monomer, Bis-GMA. Due to the enormous viscosity of this base monomer (Table 1), dilution by other compatible monomer species, decreasing overall viscosity of the resin system, is required. The most extensively employed diluent for dental resins is triethylene glycol dimethacrylate (TEGDMA, Figure 2).

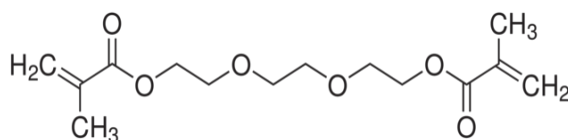
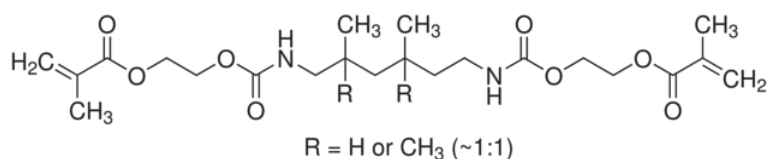


Figure 2: Example of low viscosity diluent monomer used in the formulations of matrixes of dental composites; TEGDMA.

The alternatives for Bis-GMA as a base monomer are various urethane dimethacrylate monomers (UDMA), such as 1,6-bis(methacryloxy-2-ethoxycarbonylamino)-2,4,4-trimethylhexane (Figure 3 A.), and also non-hydroxylated alternative of Bis-GMA, 2,2-bis[4-(methacryloxypolyethoxy)-phenyl]-propane (Bis-EMA, Figure 3 B.).

A.



B.

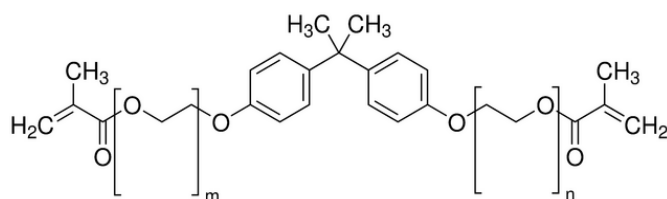


Figure 3: Examples of alternative base monomers used in the formulations of of matrixes of dental composites; A. UDMA, B. Bis-EMA.

Presence of the base monomer in the resin formulation serves to minimize polymerization shrinkage by virtue of its relatively large molecular volume and low double bond concentration. Moreover, the rigidity of the monomer backbone enhances the elastic modulus of the cured polymer. The low viscosity diluent monomer is added to provide good handling properties to the material, and also to afford improved copolymer conversion due to its greater flexibility, mobility, and smaller molecular volume [3,11,12].

## 2.2 Monomer structure and associated properties

As briefly suggested above, structure and included functionality (other than the reactive methacrylate groups) of the monomers determine the properties related to the polymerization kinetics, network morphogenesis and the mechanical performance of the cured systems. As it was stated by Stansbury [4], these properties are largely but not exclusively additive in nature when comonomer mixtures are formulated. The most important structural characteristics of the respective monomer species are briefly discussed in this chapter.

### 2.2.1 Viscosity

Initial resin viscosity is an important parameter from the perspective of the reaction kinetics, since it affects mobility of the reactive species in the polymerizing system [12]. Molecular weight and shape of the monomer molecules in the liquid state as well as its potential for intermolecular interactions determines bulk viscous flow behavior of uncured resins. Individual molecules are mutually attracted through van der Waal's forces that range from weak to relatively strong interactions. Dipole-dipole interactions represent the strongest interactions between neutral molecules. The strength of intermolecular interactions is important since these effectively make small molecules behave as larger structures [4].

Very low viscosity of TEGDMA is given by the low molecular weight and lacking hydrogen bonding donor functionalities. On the other hand, Bis-GMA exhibits dramatically high viscosities, derived from the strong hydrogen bonding between hydroxyl groups, which is exclusively intermolecular due to the rigid aromatic core structure [4,7,13]. A weaker, but still significant contribution of  $\pi$ - $\pi$  aromatic ring interactions in Bis-GMA is demonstrated by the comparison of its viscosity with those of ethoxylated bisphenol A dimethacrylate (Bis-EMA) and TEGDMA [14]. The hydroxyl groups of Bis-GMA can serve effectively as both the

hydrogen bond donors and acceptors. The urethane nitrogen in UDMA is not strongly electronegative due to the electron donation to the adjacent carbonyl. Hence, it is an ineffective hydrogen bond acceptor. UDMA hydrogen bonding interactions are weaker, and display greater intramolecular character due to the flexibility of the monomer backbone.

### 2.2.2 Reactivity

The reactivity of dental dimethacrylates goes hand in hand with the initial viscosity of the resin formulation, and structural features of monomers allowing for molecular mobility. The range of resin viscosities where optimum reactivity is observed is likely that which allows significant monomer diffusion but inhibits macroradicals translation and termination. Thus, initial resin viscosity is a major factor in controlling polymerization kinetics and the final conversion, but not the only one that controls reactivity of monomer formulations [14].

Studies on the formation of homopolymers from oligoethylene glycol dimethacrylates have shown that the reactivity of the monomers increases with increasing distance between the methacrylate groups. Due to the favorable stereochemistry, long chain and flexible dimethacrylates have also been found to exhibit relatively high degrees of double bonds conversion [15]. As both Bis-GMA and Bis-EMA contain rigid aromatic core structure, the limiting double bond conversion and overall reactivity are reduced when compared with TEGDMA or UDMA. Generally, any incremental addition of diluent monomer leads to the increase of the reactivity, polymerization rate and limiting double bond conversion in the case of all systems based on combination of base and diluent monomers [12,14,16].

*Table 1: Correlation between the molecular weight, concentration of double bonds, viscosity and glass transition temperature of dental monomers [17,18].*

Monomer	$M_w$ [g/mol]	C=C [mol/kg]	Viscosity [mPa·s]	Monomer $T_g$ [°C]
<b>Bis-GMA</b>	512.60	3.90	500 000–800 000	- 10
<b>Bis-EMA</b>	496.58	4.70	3 000–5 000	- 42
<b>UDMA</b>	470.56	4.25	5 000–10 000	- 38
<b>TEGDMA</b>	286.32	6.99	100	- 80

## 2.3 Radical polymerization of multifunctional monomers

Polymerization process of dimethacrylate monomers is a reaction triggered by free radicals, which are generated by a suitable initiation system. Double bonds of monomeric methacrylate groups are opened, generating a chain reaction the process is described by three basic steps: initiation, propagation and termination. An active center is created when the free radical attacks the  $\pi$ -bond of a monomer molecule. Propagation involves growth of the polymer chain

by rapid sequential addition of a monomer to the active center. The polymer can either grow linearly by reaction with monomers, leaving unreacted pendant double bonds, or grow three-dimensionally by reacting with other chains, creating crosslinks [19].

### 2.3.1 Aspects of the polymerization of multifunctional monomers

The process of multifunctional network formation exhibits anomalous bulk behavior, especially with respect to reaction kinetics. This includes auto-acceleration and auto-deceleration, limiting double bond conversion, unequal functional groups reactivity, trapping of free radicals, and reaction-diffusion-controlled termination and propagation mechanisms [20]. The complexity is caused by the fact that the mobility of the reacting medium varies as the polymerization proceeds. At very low double bonds conversions, propagation and termination reactions are chemically controlled. However, as the network forms, segmental movements of the macroradicals are restricted. At the gel point, mobility restriction mostly affects the radicals located on the growing chains, whereas smaller molecules can still diffuse easily through the polymerizing system. As a consequence, the rate of bimolecular termination decreases while new growth centers are still created by initiation. Concentration of free radical in the system rapidly increases, which results in a rapid increase of the polymerization rate,  $R_p$ . This has been termed auto-acceleration. As the reaction progresses, the environment becomes even more restricted along with the diminishing concentrations of residual reactive groups as the reaction proceeds. Thus, propagation reaction also becomes diffusion-controlled, resulting in the significant decrease of  $R_p$ . The decline in rate has been called auto-deceleration. The diffusion-controlled kinetics of these polymerizations leads limited degree of conversion [12,21]. Another consequence of diffusion-controlled kinetics is the entrapment of free radicals in the polymer network, sometimes termed as the monomolecular termination. However, if the mobility of the system increases again (e.g. by swelling or temperature increase above glass transition), trapped radicals become capable of reacting with remaining double bonds and thus, conversion may increase [22].

Considering multifunctional methacrylate monomers, diffusion-controlled termination dominates throughout most of the polymerization (beginning mostly as early as 2 % of double bonds conversion). In the restricted environment, radicals are unable to segmentally move and instead, as it was stated by Lovell *et. al.* [12], propagate through unreacted monomer and pendant double bonds in order to diffuse toward each other and terminate. This termination mode is called diffusion-controlled termination, and within this regime, propagation ( $k_p$ ) and termination ( $k_t$ ) kinetic constants are unchanging and related to each other through a reaction-diffusion proportionality constant,  $R$ , and the concentration of double bonds:

$$k_t = Rk_p[M] \quad (1)$$

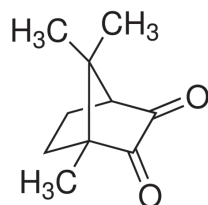
In the equation 1,  $[M]$  is the concentration of double bonds [12,23]. Value of the proportionality constant typically ranges between 2 and 3 for dimethacrylate homopolymerizations.

### 2.3.2 Photo-polymerization

Light-activated polymerization is nowadays a widely accepted mode for the curing processes required with a wide range of applications including dental restoratives. The photo-polymerization technology is based on the use of photo-reactive systems suited to absorb a light irradiation of the appropriate wavelength and to produce primary radical species able to convert a pool of multifunctional monomers into a crosslinked network. UV induced polymerization is one of the most efficient methods for the generation of highly crosslinked polymers in many industrial areas (e.g. coatings, adhesives).

Success factors of photo-initiators are linked to high absorptivity in the spectral region corresponding to the irradiating lamp emission, high efficacy in terms of the quantum yield for radical formation and high reactivity of the monomer formulation, good solubility in the curable medium, low odor and toxicity and good storage stability. These factors along with choice of photo-initiator concentration permit a high degree of external control over the photo-polymerization process. A photo-initiator is a molecule that can absorb light and as a result, either directly or indirectly generates a reactive species that can initiate polymerization. Considering the adverse health effects of UV light for oral soft tissues, visible light induced radical polymerization had fast acceptance as the curing method in the field of prosthetic dentistry. Dart and Nemecek invented the system for visible-light photo-activation that contains  $\alpha$ -diketone and tertiary amine in 1971 (Imperial Chemical Industries Co. Ltd., UK). This invention opened new possibilities in the field of visible light-curing composites [24,25].

A.



B.

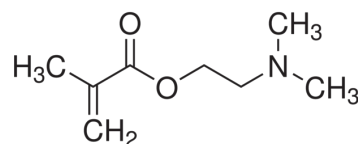


Figure 4: Structure of the most commonly used photo-initiator system, combination of: A. photosensitizer, 2,3-bornanedione (camphorquinone, CQ); B. photo-reducing agent, dimethylaminoethyl methacrylate (DMAEMA).

Photosensitizers commonly possess a carbonyl group, the non-bonding electrons of which can be promoted into a  $\pi^*$  anti-bonding orbital by absorption of light of the appropriate wavelength. This leads to a production of a pair of free radicals. The proton abstraction type of initiation occurs with 2,3-bornanedione (camphorquinone, CQ, Figure 4 A.) from a labile source. A co-initiator is a separate compound that does not absorb light, but interacts with an activated photo-initiator molecule to produce reactive radical species. In the case of dental restoratives containing CQ, a tertiary amine photo-reductant (e.g. DMAEMA, Figure 4 B.) is used as the co-initiator to provide the reactive radicals that initiate polymerization [25,26].

### 2.3.3 Photo-polymerization kinetics

Simplifying assumptions are commonly made in the development of equations in chemical kinetics. This concerns either an assumed or a demonstrable balance in rate processes between the production and extinction of intermediate molecular species.

Regarding the Lambert-Beer law, light is attenuated with increasing cross-sectional distance from the irradiated surface as a result of light absorption and scattering caused by fillers or other additives, leading to a limited depth of cure. The following equation is considering the thin film approximation in the Lambert-Beer law, relating the absorbed to the incident light intensity. The absorbed light intensity is then expressed as:

$$I_a = \varepsilon I_0 [C_s] \quad (3)$$

In the equation,  $\varepsilon$  expresses the extinction coefficient of the photo-initiator (molar absorptivity),  $[C_s]$  is the initiator concentration and  $I_0$  is the incident light intensity per unit area. The rate of production of primary free radicals from the photosensitizer ( $R_r$ ) can be formally expressed by following formula:

$$R_r = 2\phi \cdot I_a, \quad (4)$$

Where  $I_a$  is the light intensity absorbed by the photosensitizer across a thickness element  $\delta d$  and  $\phi$  is the quantum yield for initiation (number of propagating chains produced per number of photons absorbed by the system). The factor 2 is strictly optional and it is used when two radicals are generated for each photosensitizer molecule [19,27]. Detailed kinetic analysis of the individual activation steps, using camphorquinone/tertiary amine photopolymerization system, was made by Cook [28] and later re-interpreted by Watts [29]. Following expression for  $R_r$  includes mechanistic quantities of the reaction components involved in the efficient photo-activation process:

$$R_r = \beta k_a [A] \cdot [CQ_T^*] \quad (5)$$

In the equation,  $\beta$  expresses the fraction of excited state complex forming free radicals, and  $k_a$  is the rate constant for the exciplex formation from reaction of amine and triplet  $CQ^*$ . If the additional steady-state assumption is made that the rates of production and consumption of initiator radicals rapidly becomes equal, then the rate of production of primary free radicals from the photosensitizer,  $R_r$ , is equal to the rate of initiation,  $R_i$ . This assumption presumes a concentration of photo-reductant to be present at the concentration that matches that of the photo-initiator. For dimethacrylate based resin systems, this assumption is suitable due to the gelation that occurs at low degree of double bond conversion. Thus, it can be assumed that the photosensitizer and resultant free radicals do not diffuse rapidly [19,28,29].

Polymerization rate is given by the sum of rates of initiation and propagation ( $R_i$ ,  $R_p$ ), since both of the steps consume monomer. However, the initiation rate is relatively insignificant

compared with the rate of propagation and can be neglected (i.e. when the initiator concentration is low; the reaction is monitored in the dark phase after short irradiation), so:

$$-\frac{d[M]}{dt} = R_p = k_p[M^*] \cdot [M] \quad (6)$$

In the equation,  $[M]$  is the monomer concentration and  $[M^*]$  is the total concentration of all chain radicals [19,29]. The equation assumes the equal reactivity of the monomeric and pendant functional groups. The determination of actual polymerization rate coefficients ( $k_p$ ,  $k_t$ ) is difficult due to the complicated behavior of the reaction with respect to the kinetics, especially the early onset of the auto-acceleration. Values of the rate coefficients are often thought as a sum for the different coexisting radical populations contributing to propagation and termination [27,30]. The conversion dependences of polymerization rate coefficients are obtained under special assumptions, including exclusively bimolecular termination.

Due to the mentioned reaction trends, polymer radicals can be broadly classified into three populations: free radicals that are not attached to the network, radicals attached to the loosely crosslinked portion of the network so that they are spatially restricted but still mobile, and trapped radicals that are surrounded by dead polymer chains without possibility for further propagation or termination [27–31]. Within very densely crosslinked networks, the trapped radicals are eliminated from the further propagation. Thus, one may consider two types of termination reactions. The way by which the termination in the polymerizing crosslinking system occurs depends mainly on the degree of double bond conversion.

The simplified bimolecular termination model has been extensively used for the estimation of the polymerization rate coefficients. If a steady-state assumption is again made that the concentration of polymer radicals rapidly attains a constant value, it is equivalent to say that rates of initiation and normal bimolecular termination are equal, and hence:

$$R_t = -2k_t[M^*]^2 \quad (7)$$

For classical bimolecular termination behavior, one would expect  $R_p$  to scale with  $R_i$  to the  $\frac{1}{2}$  power ( $\alpha = 0.5$ ). Rearrangement and substitution in the equation 6 yields:

$$R_p = \frac{k_p}{k_t^{1/2}} [M] \cdot \left(\frac{R_i}{2}\right)^{\alpha} \quad (8)$$

The expression for  $R_i$  in the equation 4 may be substituted for  $R_i$  in the equation 7 to obtain:

$$R_p = -\frac{d[M]}{dt} = k_p[M] \cdot \left(\frac{\phi \cdot I_a}{k_t}\right)^{0.5} \quad (9)$$

The equation shows that the rate of polymerization is proportional to the square root of the absorbed light irradiance and hence, proportional to the square root of the photo-initiator concentration [19,27–29].

An alternative path of termination involves chain transfer. Increased viscosity suppresses the bimolecular termination at the benefit of termination by transfer. This reaction provides additional mobility to the radical sites by influencing the kinetic chain length, reducing the lifetime of the radicals and hence, reducing the polymerization rate [30]. However, inherent chain transfer termination mode is negligible considering dimethacrylate monomers and thus, the methacrylate systems do not conform to the square root dependence (Equation 8). The less than  $\frac{1}{2}$  dependence is attributed to the chain length dependent termination effects (long, entangled and highly crosslinked chains exhibit slow termination rate).

## **2.4 Special features of multifunctional network formation**

Understanding the mechanisms of network formation by various multifunctional monomers requires comprehensive approach, especially because the process exhibits abnormalities related to increasing viscosity, decreasing mobility and the heterogeneous distribution of reacting species along with reaction progress. Once more, this includes auto-acceleration, auto-deceleration, limiting functional group conversion (reaction-diffusion-controlled termination), and varying pendant double bonds reactivity.

In general, polymerization kinetics shows changes in the concentrations of the reactive species throughout the polymerization. Consumption of functional groups is greatest during the auto-acceleration period and slows down during the auto-deceleration period. Furthermore, it is necessary to take account the structural parameters of the individual monomer species with respect to the anomalous pendant double bond reactivity and mobility of structurally distinct monomer species throughout the polymerizing system. Chain polymerization of the multifunctional monomers leads to the formation of pendant double bonds. Further propagation may proceed via three different ways. This involves addition of the next monomer molecule, extending the length of macroradical chain and intramolecular or intermolecular attack of the radical site to the pendant. Intramolecular crosslinking leads to the cyclization reaction, whereas intermolecular crosslinking leads to the network formation [14,30,32–35]. The Flory-Stockmayer theory has been used to predict gel point conversions in the systems, having a relatively low density of crosslinks (systems are assumed to be homogeneous and functional groups are assumed to possess equal reactivity). However, as it was experimentally proven by Dušek [36], if the fraction of crosslinking monomers increases, the conversion at the gel point is significantly greater than predicted by the Flory-Stockmayer theory. The explanation of this behavior lies in the unequal reactivity of the functional groups. The effect of cyclization on the process of network formation has been observed experimentally, including the shift of the gel to the higher conversion than predicted theoretical value. Higher local conversion is promoted because the mobility of the system is not restricted when ineffective crosslinks are formed and thus, the gel point conversion is delayed on the conversion scale.

Initially, propagation through intramolecular cyclization is promoted due to an enhanced apparent reactivity of the pendant double bond on the same chain when compared with monomeric functional groups. This is related to a larger concentration of pendants in the

vicinity of the radical site. Initial extensive cyclization leads to the formation of the compact structures, so called mono-chain microgel domains [36]. After that, the apparent reactivity of the pendant double bonds is decreased due to the various kinds of steric hindrance effects, preventing either inter or intramolecular crosslinking (i.e. excluded-volume effects). This causes a strong diffusion control of the reaction since the groups located in the interior of a branched polymer has less opportunity to react than those located on the periphery [36–41]. Thus, a concentration of the accessible pendant functional groups is considerably decreased when a higher degree of conversion is reached, and the overall reactivity of pendant functional groups decreases [38]. Further reaction (macro-gelation) occurs by the chemical joining of initially formed microgels. Thus, polymerization proceeds by the mechanisms completely different from those leading to branching trees (the postulate of the classic Flory-Stockmayer theory). It may rather resemble chemical aggregation of colloidal particles [36].

The choice of monomer system composition and curing conditions both have the potential to affect the gel point to a large extent. It takes only seconds for an individual chain to fully grow from initiation to termination. Primary chains having large molecular weight and containing numerous pendant double bonds are instantaneously formed at the beginning of the polymerization. Due to a high dilution of chains at the beginning of the reaction and relatively slow diffusion compared with fast propagation, rapid intramolecular reactions between propagating radical and pendant double bonds at a vicinity are favored. Since the cyclization reactions of flexible monomers produce ineffective crosslinks, their occurrence delays a gel point conversion when compared with monomers that form primarily effective crosslinks. The number and concentration of reactive functional groups also influence the appearance of the gel point [4,35,41]. Beyond the gel point, the transition from chain-length dependent termination to reaction-diffusion-controlled termination occurs. Consequently, propagating chain radicals rely on spatial extension based on the propagation reaction to encounter other radical and terminate. Resin systems that present higher initial viscosities before polymerization tend to enter this transition to reaction-diffusion-controlled kinetics at an earlier stage of conversion and thus, reach a lower limiting conversion [21,33,42,43].

Unlike the gel point, which is a well-defined point on the conversion scale, vitrification is strongly dependent on the reaction conditions since it is determined by mobility restrictions that are affected by factors such as temperature and free volume. The decrease in free volume, associated with mobility restrictions of a polymer chain segments typically reduce the reaction rate by orders of magnitude, making it difficult to achieve higher values of the glass transition temperature [4,44–46]. Dimethacrylate networks are thought to be formed with a certain degree of heterogeneity, which implies a very wide variations in segmental chain mobility and relaxation times. Thus, the transition from the rubbery to the glassy state occurs over a range of functional groups conversions. Due to the process of microgel formation and aggregation, bulk vitrification does not occur until the crosslink density of the regions between the microgel domains reaches the threshold of significant mobility restriction. Therefore, the glass transition temperature should be considered as an average value, but not as a point at which the whole polymer changes from the rubbery to the glassy state [96–100]. With the transition to the bulk glassy state, the rate of polymerization slows by several orders of magnitude (i.e. auto-deceleration).

### **3 AIM OF THE THESES**

The main aim of this thesis is the investigation of kinetics and mechanisms of dimethacrylate copolymer networks morphogenesis with the ultimate goal to achieve defined network structures with maximum reproducibility. The base for understanding the controlled structure formation is provided by examination of the network-formation kinetic profiles. The kinetics of the polymerization is studied using resin systems containing structurally distinct monomer species, different comonomer molar ratios and varying concentration of photo-initiation system.

Furthermore, the relationship between supra-molecular structure, viscoelastic behavior and thermal stability of dimethacrylate networks is investigated. The relationship between the supra-molecular structure of the networks, storage modulus and damping behavior within a given temperature range is quantified. The differences in thermal stability are interpreted in terms of degradation mechanisms, which are highly dependent on the structural characteristics of a corresponding resin system.

## 4 EXPERIMENTAL PART

This chapter provides detailed description of materials and methods of characterization used to fulfill the aims of this thesis. The choice of materials includes the most commonly employed monomers and photo-initiation reagents in the formulations of current resin-based composites and dental adhesives. For the purpose of dynamic-mechanical analysis, experimental bodies pre-polymerized by heat-induced polymerization were employed to avoid thermally induced post curing during testing. Simple model resins mixtures are taken into consideration to fully understand the complex process of multifunctional networks formation.

### 4.1 Materials

*Table 2: Materials used for the preparation of studied resin systems.*

Full name	Abbreviation	Molecular weight Specific gravity	Supplier
Bisphenol A-glycidyl methacrylate	Bis-GMA	512.60 g/mol 1.16 g/ml	Esschem Europe Ltd
Ethoxylated Bisphenol A dimethacrylate (3 units of ethoxylation)	Bis-EMA	496.58 g/mol 1.12 g/ml	Esschem Europe Ltd
Urethane dimethacrylate	UDMA	470.56 g/mol 1.13 g/ml	Esschem Europe Ltd
Triethylene glycol dimethacrylate	TEGDMA	286.32 g/mol 1.09 g/ml	Esschem Europe Ltd
Camphorquinone	CQ	166.22 g/mol /	Sigma Aldrich / Merck
(Dimethylamino)ethyl methacrylate	DMAEMA	157.21 g/mol 0,93 g/ml	Sigma Aldrich / Merck
Dicumyl peroxide	DCP	270.37 g/mol /	Sigma Aldrich / Merck

## 4.2 Experiments overview

This chapter summarizes the way of preparation of different resin formulations and curing procedures of experimental bodies characterized by the aforementioned experimental methods. From the manufacturer, the monomers with a high purity grade were obtained (maximum content of 100 ppm of MeHQ as an inhibitor), and were used as received without further purification. Composition and designation of all of the studied resin formulations are summarized in Table 3 (light cured samples for DPC, FTIR and TGA analysis) and Table 4 (heat cured samples for DMA and FTIR analysis).

### 4.2.1 Photo-polymerization kinetics (DPC)

Prior to mixing, the monomers (see Chapter 4.1) were heated up and kept at 60 °C for one hour to reduce its viscosity. Then, the monomers were dosed in appropriate molar ratios into the light-impermeable vials and mixed by means of magnetic-stirring for one hour. After that, the components of photo-initiation system were added in the appropriate molar concentrations and dissolved by mixing the system for another hour. The same molar concentrations of camphorquinone (CQ) and (Dimethylamino)ethyl methacrylate (DMAEMA) were added into the resin mixtures in order to keep the equimolar ratio of photo-sensitizer and photo-reductant to obtain comparative results. Composition and designation of all of the studied resin formulations are summarized in the Table 3. Prior to measurement, the resin systems were stored in the fridge at 5 °C. Before the weighing of the samples into the aluminum pans, the resins were kept in thermostat at 37 °C for 60 minutes. The measurement was carried out immediately after the placement into the aluminum pans.

The rate of polymerization ( $R_p$  [ $\text{mol}\cdot\text{l}^{-1}\cdot\text{s}^{-1}$ ]) in a unit of fractional vinyl conversion per second can be calculated (equation 10) by measuring the heat flow ( $h$ , [W/g], using the appropriate resin density,  $\rho$ ) at a given temperature and dividing the value by the specific heat of the reaction,  $\Delta H_0^{\text{theor}}$  (54,82 kJ/mol for methacrylate double bond, considering the limiting conversion of functional groups in the polymerizing system) [47].

$$R_p = -\frac{d[M]}{dt} = \frac{dH/dt}{\Delta H_0^{\text{theor}}} = \frac{h \cdot \rho}{\Delta H_0^{\text{theor}}} \quad (10)$$

Based on the assumption that the heat generated during the polymerization process is proportional to the percentage or concentration of the reacted functional groups, the extent of polymerization can be calculated. Integrating the heat flow curve versus time provide the vinyl double bond conversion,  $P_{C=C}$  [%]:

$$P_{C=C} = \frac{\int_0^t dH/dt}{\Delta H_0^{\text{theor}}} = \frac{\Delta H_t}{\Delta H_0^{\text{theor}}} \times 100 \quad (11)$$

Monitoring of the polymerization process was carried out using DSC 2920 calorimeter (TA Instruments, USA) equipped with the extension for photo-calorimetry. Two aluminum pans were placed in the sample holder of DSC furnace. Resin samples weighing approximately

10 mg ( $N = 5$  for each resin formulation) were placed in one pan, while the other pan was left empty as a reference. Resin formulations were tempered at 37 °C in the DSC furnace for 1 minute, and then irradiated by light emitted from the mercury-xenon gas discharge lamp (Oriel, Newport) for 10 minutes, using FSQ-BG 40 filter (Newport) with the maximum transmission wavelength of 470 nm. Measurements were carried out at constant temperature of 37 °C under nitrogen atmosphere (70 ml/min flow) to avoid the formation of oxygen inhibition layer. Heat flow [mW] vs. time [s] was continuously recorded ( $N = 5$  for each resin formulation). Conversion of double bonds and polymerization rate were calculated based on the measured heat flow profiles according to equations 10 and 11.

#### **4.2.2 Determination of degree of double bonds conversion (FTIR)**

A droplet of unpolymerized resin was placed over the diamond crystal and the absorbance peaks before curing were obtained in the attenuated total reflection (ATR) mode. The cured resin droplets removed from the aluminum pans after DPC analysis were used as the cured specimens to determine the decrease of intensity of aliphatic C=C peak at 1637  $\text{cm}^{-1}$  after curing. The measurement was performed immediately after the DPC analysis. The cured resin droplets were laid over the crystal and fixed by the sample holder. In the same way, the degree of double bonds conversion was determined for the heat-cured samples. The absorbance peaks were obtained for un-polymerized resins and the polymerized droplets, that had been cured simultaneously with the experimental bodies intended for the DMA analysis in the silicone rubber mold. After curing, the resin droplets were treated the same way as the experimental bodies, and the measurement was performed prior to DMA analysis.

FTIR spectra of cured and uncured resin samples ( $N = 5$  for each resin formulation) were obtained using Tensor 27 spectrometer (Bruker, USA) in ATR mode with diamond crystal, set up to 64 scans and 4  $\text{cm}^{-1}$  resolution. The percentage of unreacted double bonds was determined from the ratio of absorbance intensities of aliphatic C=C peak at 1637  $\text{cm}^{-1}$  against internal standards before and after curing of the specimens. As internal standards, aromatic peak at 1608  $\text{cm}^{-1}$  for Bis-GMA and Bis-EMA based systems, carbonyl peak at 1720  $\text{cm}^{-1}$  for neat TEGDMA (PEGDMA) systems, and secondary amine group at 1527  $\text{cm}^{-1}$  for UDMA system were used. The same resin systems were analyzed by FTIR and DPC to compare the degree of double bonds conversion obtained by both methods.

#### **4.2.3 Kinetics of thermal degradation (TGA)**

The resin formulations for the purpose of TGA analysis were mixed by the same manner as for the colorimetric analysis. Afterwards, the resin systems were cured in the form of discs (5 mm diameter, 1 mm height). The samples were prepared by pouring the resin into the silicon rubber mold, tempered at 37 °C for 15 minutes, covered with mylar strips and put into the light-curing chamber Targis Power (Ivoclar Vivadent, Schaan, Liechtenstein). The source consists of 75 W halogen lamp emitting radiation between 400 and 580 nm and has maximum peak at 470 nm. The samples were irradiated for 4 minutes on each side. The measurement was carried out immediately after the curing.

Kinetics of degradation process was monitored using thermo-gravimetric analyzer Q 500 (TA Instruments, USA). Cured resin samples about 20 mg each were used ( $N = 3$  for each resin formulation). First, the specimens were held at 50 °C for 2 minutes for the temperature stabilization throughout the sample bulk and then heated up to 600 °C. The measurements were performed at 10 °C/min heating rate under a constant nitrogen flow of 60 ml/min. Sample mass vs. temperature were continuously recorded. The same resin systems were analyzed as in the case of DPC. TGA analysis was performed in order to characterize the systems cured under the same conditions while using structurally different monomer species. The measurements were partially affected by the thermally-induced post-curing. However, in agreement with the conclusions reported in the literature [48–50], the data obtained by the characterization of kinetics of thermal degradation process provide valuable insight into the structural parameters of photo-cured dimethacrylate networks.

*Table 3: Summary of the light-cured resin systems characterized by DPC, FTIR and TGA.*

<b>Designation</b>	<b>Monomer formulation</b>	<b>Concentration of photo-initiators</b>
Bis-GMA	Neat monomer	1.4 mol. %
Bis-EMA	Neat monomer	1.4 mol. %
UDMA	Neat monomer	1.4 mol. %
TEGDMA	Neat monomer	1.4 mol. %
Bis-GMA:TEGDMA 2:1	Molar ratio 2:1	1.4 mol. %
Bis-GMA:TEGDMA 1:1	Molar ratio 1:1	1.4 mol. %
Bis-GMA:TEGDMA 1:2	Molar ratio 1:2	1.4 mol. %
Bis-EMA:TEGDMA 2:1	Molar ratio 2:1	1.4 mol. %
Bis-EMA:TEGDMA 1:1	Molar ratio 1:1	1.4 mol. %
Bis-EMA:TEGDMA 1:2	Molar ratio 1:2	1.4 mol. %

#### **4.2.4 Viscoelasticity of the networks (DMA)**

The experimental bodies were cured in the silicon rubber molds providing the rectangular shape of 40 x 4 x 2 mm. The resins intended for heat curing were activated by addition of dicumyl peroxide in the concentration of 1.4 mol. % into the monomer mixture. The resins were poured into the silicon rubber mold and then cured in the vacuum oven at 120 °C for 90 minutes and post-cured at 220 °C for another 90 minutes. The cured samples were allowed to cool to the room temperature for 60 minutes, rinsed with acetone in order to remove oxygen inhibition layer and the overflows were trimmed. The samples were stored in the thermostat at 37 °C for 24 hours prior to the analysis. Only heat-cured samples were used for the purposes of DMA to avoid thermally-induced post-curing during the analysis. The method

of curing is irrelevant from the clinical point of view, but is instrumental for an understanding of the viscoelastic behavior of dimethacrylate networks.

The analysis was performed using DMA RSA G2 solid analyzer (TA Instruments, USA). Simply supported mode was preferred for dimethacrylate glassy networks in order to avoid buckling effects. Bending load was applied at 1 Hz frequency in a three-point bending 25 mm mode at a dynamic scan rate of 5 °C/min and 0.01 % deformation. Rectangular samples ( $N = 5$  for each resin formulation) were placed into the analyzer geometry and the viscoelastic parameters were recorded within the temperature range of 40–250 °C.

*Table 4: Summary of heat-cured resin systems characterized by DMA and FTIR.*

<b>Designation</b>	<b>Monomer formulation</b>	<b>Concentration of initiator</b>
Bis-GMA	Neat monomer	1.4 mol. %
Bis-EMA	Neat monomer	1.4 mol. %
UDMA	Neat monomer	1.4 mol. %
TEGDMA	Neat monomer	1.4 mol. %
Bis-GMA:TEGDMA 2:1	Molar ratio 2:1	1.4 mol. %
Bis-GMA:TEGDMA 1:1	Molar ratio 1:1	1.4 mol. %
Bis-GMA:TEGDMA 1:2	Molar ratio 1:2	1.4 mol. %
Bis-EMA:TEGDMA 2:1	Molar ratio 2:1	1.4 mol. %
Bis-EMA:TEGDMA 1:1	Molar ratio 1:1	1.4 mol. %
Bis-EMA:TEGDMA 1:2	Molar ratio 1:2	1.4 mol. %

## 5 RESULTS AND DISCUSSION

### 5.1 Morphogenesis of dimethacrylate network

As it was discussed in the theoretical part, the process of tetra-functional networks morphogenesis is extremely complex, especially with regards to the reaction kinetics. The number of interesting morphological peculiarities arise from the differences in the structure of the employed monomer species, the ratio of different comonomers in the resin formulations, length of the monomer backbone, concentration of initiator and outer conditions (i.e. temperature and light intensity). The effects directly related to the formulation of resin systems are further studied in this chapter.

The DPC kinetic profiles provide a lot of important parameters, including a maximum rate of polymerization ( $R_{p, \max}$ ), position of the  $R_{p, \max}$  on the conversion scale (i.e. onset of auto-deceleration), a degree of limiting double bond conversion and a basic idea about mechanisms of network morphogenesis. Vinyl conversion was also measured by FTIR to compare the results of both methods. These findings were further discussed in relation to the data obtained from TGA analysis (i.e. kinetics of thermal decomposition).

#### 5.1.1 Effects of monomer structure

The structural parameters of different monomer species clearly affect polymerization kinetics to a vast extent. The curves (Figure 5 and 6) show considerable differences in curing behavior despite the constant temperature, molar concentration of photo-initiators and light intensity of the curing unit. Table 5 shows the key kinetic parameters for homopolymerization of studied monomers. The results of limiting degree of double bond conversion as determined by DPC and FTIR differ in the range of 2–5 %. These differences are associated with the sensitivity and resolution of both methods, neglectation of other possible reactions generating heat during DSC experiments beyond consumption of vinyl groups, weighing errors, and possible post-cure when the droplet of the cured resin was moved from DPC measuring cell to FTIR apparatus.

*Table 5: Mean and standard deviation values of maximum rate of polymerization ( $R_{p, \max}$ ), degree of conversion ( $P_{C=C}$ ) at  $R_{p, \max}$  and limiting degree of conversion ( $P_{C=C}$ ) as determined by DPC and FTIR; neat monomers.*

Designation	$R_{p, \max}$ [mol/l·s]	$P_{C=C}$ at $R_{p, \max}$ [%]	$P_{C=C}$ [%], DPC	$P_{C=C}$ [%], FTIR
Bis-GMA	0.0156 (0.0011)	4.67 (0.32)	29.58 (0.45)	33.16 (0.69)
Bis-EMA	0.0452 (0.0014)	10.19 (0.06)	56.90 (1.45)	52.18 (1.29)
UDMA	0.1047 (0.0050)	13.19 (0.75)	57.80 (1.94)	55.14 (0.75)
TEGDMA	0.0448 (0.0015)	35.15 (1.27)	68.68 (1.17)	63.17 (1.32)

Among others, neat Bis-GMA monomer shows lowest  $R_{p, \max}$  (Figure 5), earliest onset of auto-deceleration period and lowest degree of double bond conversion. Dramatic increase in reaction rate in the early stage of polymerization is attributed to strong diffusion limitations of the termination (i.e. immediate gelation). However, since the initial resin viscosity is very high in case of Bis-GMA, the propagation reaction (i.e. movement of remaining monomers) becomes restricted also very early within the conversion scale ( $P_{C=C}$  at  $R_{p, \max} = 4.67\%$ ). Strong mobility restrictions associated with the vitrification cause very low limiting degree of conversion (29.58 % DPC, 33.16 % FTIR). The explanation of these findings relies in the potential for very strong and mostly intermolecular hydrogen bonding between monomers, causing a decreased mobility of monomer molecules during the polymerization, and rigid aromatic structure of Bis-GMA backbone with a large radius of gyration, decreasing the mobility of pendant functional groups during polymerization. The accessibility of pendant functional groups is severely limited due to the steric hinderance effects.

On the contrary, Bis-EMA (ethoxylated variant of Bis-GMA) shows different kinetic behavior with respect to the degree of conversion at  $R_{p, \max}$  ( $P_{C=C}$  at  $R_{p, \max} = 10.19\%$ ) and limiting conversion (56.90 % DPC, 53.18 % FTIR). Lacking hydrogen-bonding donor sites (substitution of 2-hydroxypropyl groups between aromatic core and methacrylate groups in Bis-GMA for flexible ethoxylated linkages in Bis-EMA) results in much lower initial viscosity by orders of magnitude (Table 1), allowing for a greater mobility in the bulk of the reacting system. The ether groups of Bis-EMA cannot participate in hydrogen bonding with each other. Thus, the main factor that limits the reaction progress is the rigid aromatic core structure. Similar conclusions, relating the differences of polymerization behavior of structurally similar monomer species to the potential for physical interactions, were reported in the literature [7,12,14,51].

Different reaction behavior was observed in case of UDMA monomer. The highest reaction rate was observed in case of UDMA homopolymerization, however, the degree of conversion at  $R_{p, \max}$  ( $P_{C=C}$  at  $R_{p, \max} = 13.19\%$ ) and especially degree of limiting conversion (57.80 % DPC, 55.14 % FTIR) are comparable with the same kinetic parameters of Bis-EMA homopolymerization. Lower initial viscosity and higher reaction rate allowed access to higher conversion levels. As it was shown by Lemon *et al.* [13], Khatri *et al.* [52] and Barszczewska-Rybarek [53], lower viscosity of UDMA based resins is related to the fact, that hydrogen bonding interactions associated with the urethane functionalities are significantly weaker than those associated with hydroxyl functionalities and may poses more intramolecular character. The higher reactivity of UDMA monomer is related to the flexible structure of its monomer backbone, including aliphatic core, urethane functional groups, and ethoxylated linkages between methacrylate functional groups. Also, as it was suggested by Sideridou *et al.* [18,33], the reactivity of UDMA may be related to other factors, including abstraction of labile hydrogen atoms from the carbamate groups. Due to these chain transfer reactions, caused by  $-NH-$  groups, the mobility of radicals increases and an alternative path of the propagation reaction is offered. These are the reasons why propagation proceeds further before it becomes diffusion-controlled. Furthermore, the flexibility of the monomer backbone is also associated with better accessibility of pendant functional groups in the vicinity of the radical site. This may, however, increase the reactivity and promote higher methacrylate groups conversion,

but the formation of primary cycles does not contribute to the effective crosslink density. The occurrence of primary cyclization reactions in UDMA homopolymers was reported by Achilias *et al.* [49] and later by Vouvoudi *et al.* [50].

Bimodal profile of reaction rate is evident in case of TEGDMA homopolymerization. This phenomenon was described by several studies [12,14,35] and has been interpreted in terms of low monomeric viscosity and primary cyclization. Bimodal profile is related to a delayed onset of diffusion-controlled termination. This effect goes hand in hand with low initial resin viscosity and extensive reactivity through primary cyclization, creating ineffective crosslinks. This behavior delays gelation and thus, the onset of auto-acceleration is also delayed. Thanks to the aforementioned parameters, especially the degree of conversion at  $R_{p, \max}$ , reached by far the highest value when compared with other monomers ( $P_{C=C}$  at  $R_{p, \max} = 35.15\%$ ) despite the highest concentration of the double bonds per unit mass. The extent of cyclization during polymerization of TEGDMA was predicted on the basis of kinetic gelation models [38,54]. Initially, primary cyclization dominates and the cycles are formed at the expense of unreacted monomers, since pendant double bonds have an increased reactivity in the localized region of the free radical. This behavior is responsible for genesis of structural heterogeneity (i.e. formation of microgel domains). As conversion increases, the probability of crosslinking also increases and the network is formed. This decrease of reactivity through primary cyclization is the result of the inaccessibility of the pendant functional groups to the radical sites as they become sterically hindered. Afterwards, the reactivity of monomeric functional groups exceeds that of the pendant groups and polymerization continues until all functional groups are inaccessible to the radicals. Based on the kinetic models, the fraction of pendant double bonds that undergo primary cyclization approaches 80 % at the beginning of the polymerization, and dominates over secondary cyclization reactions and effective crosslinking over the wide range of functional groups conversion. The probability of primary cyclization severely decreases with increasing molecular weight of the monomers, because pendant functional group is further from the propagating radical. This may be the reason of lower extent of primary cyclization reactions in the case of UDMA homopolymerizations.

Another model enabling the estimation of probability of primary cyclization with regard to the stiffness of the monomer backbone was developed by Elliot *et al.* [35]. TEGDMA pendants undergo cyclization almost three-times more often than Bis-GMA pendants under the same conditions (i.e. pendants are surrounded by the same quantity of radicals, the probability of crosslink formation is the same). This difference is given by the flexibility of the aliphatic monomer backbone when compared with stiff aromatic backbone of Bis-GMA. The probability of cyclization is the highest immediately after the formation of the pendant, when the propagating radical is in the vicinity. However, if this is prevented due to the stiffness of the monomer and a sterically unfavorable ring would be formed, the probability of primary cycle formation is fairly low. Bimodal profile was not seen in case of UDMA homopolymerization, even though the occurrence of primary cyclization reactions is also very likely to occur due to the flexibility of monomer backbone. This difference is related to the lower probability of primary cyclization [38,54] and higher initial viscosity [13], resulting in almost immediate gelation, earlier onset of auto-acceleration and steady rise of the reaction rate.

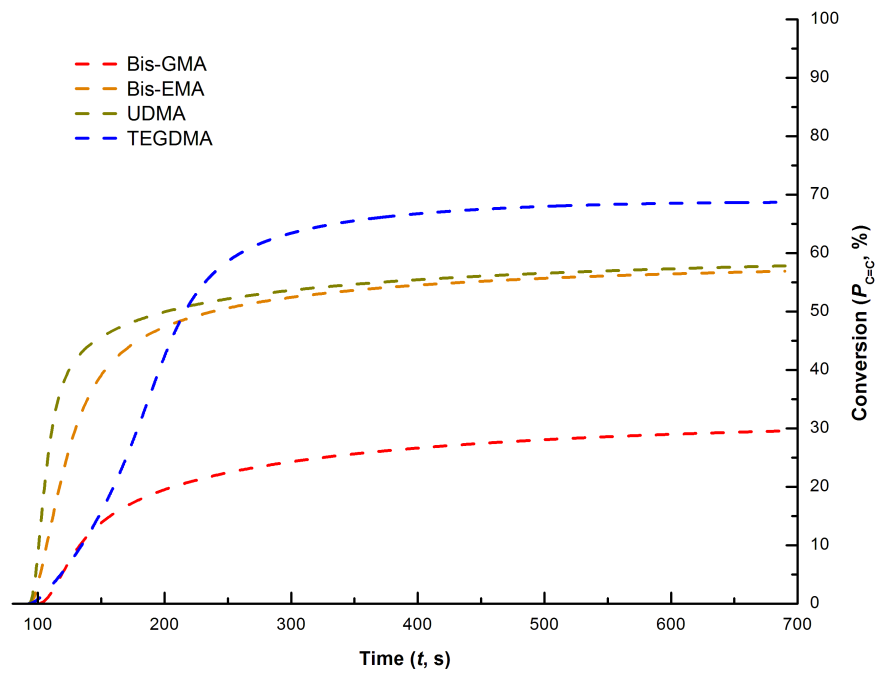


Figure 5: Photo-polymerization kinetic data, degree of double bond conversion as a function of time; neat monomers.

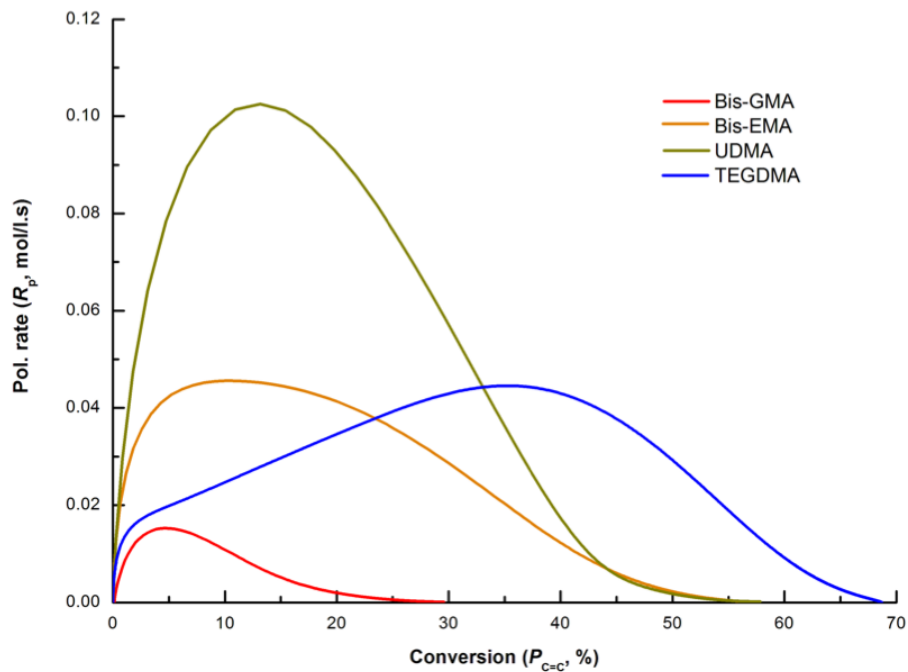


Figure 6: Photo-polymerization kinetic data, reaction rate ( $R_p$ ) normalized by the initial double bond concentration; neat monomers.

The study of thermal degradation kinetics provides a valuable information regarding the morphology of dimethacrylate networks. This may be helpful for further interpretation of the conclusions formulated on the basis of photo-polymerization kinetics, even though a post-curing is expected to occur resulting in the slight network development. Table 6 shows the threshold parameters of thermal degradation process of dimethacrylate homopolymers. Thermal decomposition is a radical depolymerization, where either end chain or random scission of the macromolecular chains occurs. As it was reported by Pielichowski *et al.* [55], in case of PMMA, end chain scission initiated at vinylidene groups is favored at low temperatures and random scission at high temperatures.

Table 6: Mean and standard deviation values of temperature where thermal degradation start ( $T_0$ ), and the first ( $T_1$ ) and second ( $T_2$ ) maximum of thermal decomposition and residual mass at 600 °C; neat monomers.

Designation	$T_0$ [°C]	$T_1$ [°C]	$T_2$ [°C]	Residual mass at 600 °C [%]
Bis-GMA	258.26 (0.72)	/	399.71 (1.22)	14.22 (0.52)
Bis-EMA	238.97 (1.23)	/	418.71 (0.34)	0.94 (0.13)
UDMA	228.40 (2.68)	331.33 (0.51)	427.46 (0.80)	0.43 (0.14)
TEGDMA	212.37 (2.89)	300.68 (0.46)	379.12 (0.99)	0.46 (0.45)

As expected for highly crosslinked polymers, thermal decomposition is complex heterogeneous process consisting of several steps. The initial loss may be associated with the degree of effective crosslinking and degree of vinyl conversion. As it was published by Teshima *et al.* [48], the initial products of pyrolysis are methacrylic acid (MA) and 2-hydroxyethyl methacrylate (HEMA) in a similar way to the degradation of PMMA. The fact that the amount of these compounds decreases with increasing conversion in the initial and second phase of thermal decomposition suggests, that MA and HEMA were generated from residual unpolymerized monomers and pendant functional groups. In a later stage of decomposition, propionic acid (PA) from the ends of polymer chains and phenol generated from a random chain scission in the final stage of decomposition were clearly identified.

In case of Bis-GMA homopolymer, degradation is completed in only one step, starting at 260 °C ( $T_0$ ), and reaching the maximum rate at 400 °C ( $T_2$ ). Similar behavior was observed in case of Bis-EMA homopolymer, but with lower residual mass (carbonization yield). As it was discussed above, the probability of primary cyclization is severely limited because of the presence of stiff and rigid aromatic monomer backbone. Due to the steric hinderance effects, these monomers are not able to react intramolecularly with the radical on the same propagating chain until several repeat units had been added and thus, resulting morphology is more homogeneous. The degradation at higher temperatures is attributed to the existence of only small number of inhomogeneities. The temperature giving the maximum rate of thermal decomposition ( $T_2$ ) is higher in case of Bis-EMA due to the higher degree of covalent

crosslinking and the fact, that the hydrogen bonding interactions in Bis-GMA are weakened abruptly due to the steady rise of the temperature [13].

In contrast, thermal degradation proceeds in two distinct steps in the case of UDMA and TEGDMA homopolymers (Figures 7, 8). The initial weight loss of TEGDMA begins at 212 °C, and the decomposition rate maxima occurred at 300 °C and 382 °C. These thresholds are slightly higher in case of UDMA, starting the degradation at 228 °C, and reaching the decomposition rate maxima at 331 °C and 427 °C. These results go hand in hand with the assumptions made on the basis of polymerization kinetics. Due to the varying reactivity of functional groups, microgel domains are created around multiple initiation sites upon exposure to polymerization light, followed by their agglomeration into clusters and their interconnections [36–39,54–57]. As it was already discussed above, at low conversions the reactivity of pendant functional groups far exceeds the reactivity of monomeric functional groups. This leads to the formation of multiple loops and highly crosslinked regions embedded in a less crosslinked matrix. In a later stage, pendant functional groups become hindered in the inner structure of the microgels and less crosslinked matrix is formed. The first degradation step reflects the degradation that originates in the loosely crosslinked regions of the network, whereas the second step is associated with the decomposition of the densely crosslinked domains. Higher thermal stability of UDMA is related mostly to the fact, that cyclization is more likely when the spacer length between methacrylic groups is smaller [35]. The lower extent of cyclization is evident from the dTGA curves (Figure 8) when the proportions of first and second degradation steps are compared. Corresponding conclusions related to the mechanisms of thermal degradation were reported in the literature, where it had been interpreted based on the determination of activation energies of the distinct phases of degradation processes [49,50,58].

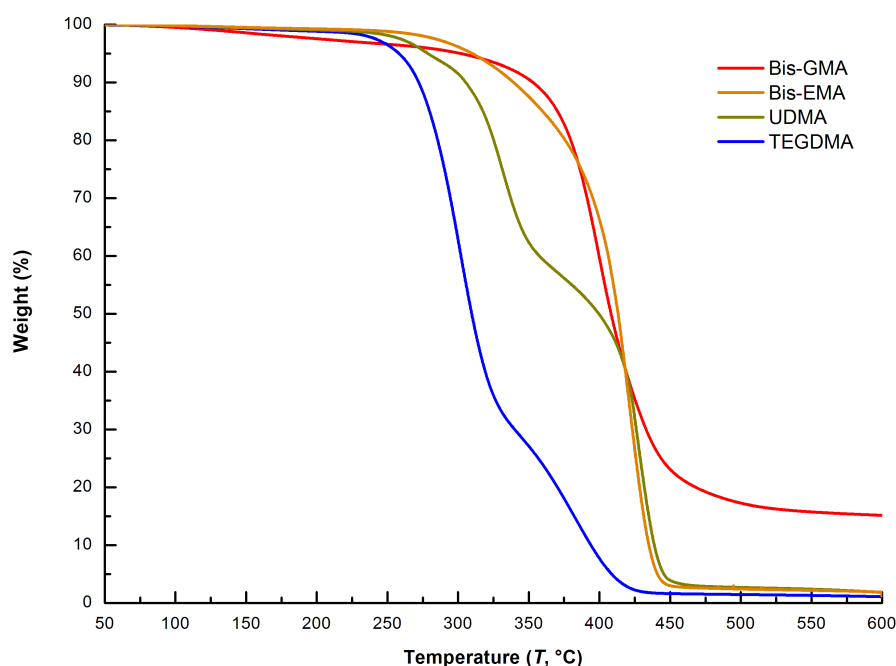


Figure 7: TGA scans, mass loss vs. temperature; neat monomers.

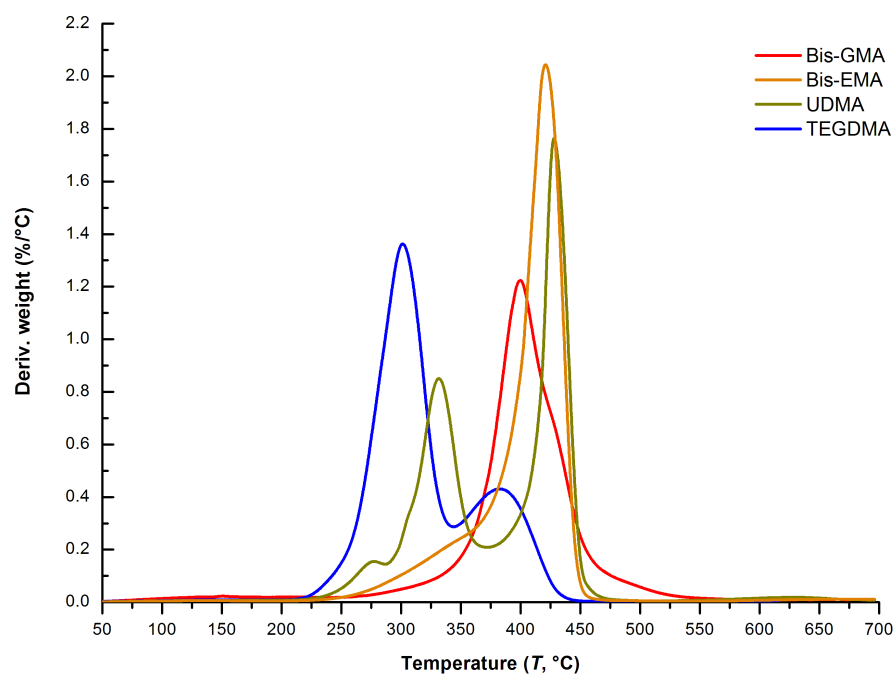


Figure 8: Derivative curves, mass loss vs. temperature; neat monomers

### 5.1.2 Effects of comonomers ratio

Synergistic effect of base and diluent monomers combination on the polymerization rate, onset of auto-deceleration and the limiting degree of double bond conversion was found in both Bis-GMA and Bis-EMA based comonomer systems with TEGDMA. Copolymerization kinetic profiles obtained at the constant temperature, molar concentration of photo-initiators and light intensity of the curing unit are shown in Figures 9–12. Table 7 summarizes the main kinetic parameters of dimethacrylate copolymerizations.

*Table 7: Mean and standard deviation values of maximum rate of polymerization ( $R_{p, \max}$ ), degree of conversion ( $P_{C=C}$ ) at  $R_{p, \max}$  and limiting degree of conversion ( $P_{C=C}$ ) as determined by DPC and FTIR; Bis-GMA/TEGDMA and Bis-EMA/TEGDMA copolymers.*

Designation	$R_{p, \max}$ [mol/l·s]	$P_{C=C}$ at $R_{p, \max}$ [%]	$P_{C=C}$ [%], DPC	$P_{C=C}$ [%], FTIR
Bis-GMA	0.0156 (0.0011)	4.67 (0.32)	29.58 (0.45)	33.16 (0.69)
Bis-GMA:TEGDMA, 2:1	0.0489 (0.0016)	9.50 (0.54)	45.78 (1.20)	42.21 (3.75)
Bis-GMA:TEGDMA, 1:1	0.0551 (0.0012)	14.91 (0.22)	55.42 (1.16)	51.42 (2.77)
Bis-GMA:TEGDMA, 1:2	0.0548 (0.0021)	20.34 (1.04)	59.22 (1.56)	57.50 (3.39)
Bis-EMA	0.0452 (0.0014)	10.19 (0.60)	56.90 (1.45)	52.18 (1.29)
Bis-EMA:TEGDMA, 2:1	0.0556 (0.0017)	22.74 (0.70)	63.44 (1.99)	60.05 (0.70)
Bis-EMA:TEGDMA, 1:1	0.0527 (0.0029)	26.86 (0.53)	64.44 (0.85)	61.83 (1.17)
Bis-EMA:TEGDMA, 1:2	0.0490 (0.0025)	30.70 (0.75)	65.44 (0.22)	62.73 (0.47)
TEGDMA	0.0448 (0.0015)	35.15 (1.27)	68.68 (1.17)	63.17 (1.32)

Copolymerization kinetic profiles show intermediate behavior between those of the corresponding monomers. In the case of Bis-GMA based copolymers, dramatic increase of reactivity was observed, because the mobility of monomers in the reacting system increased. This is due to the following factors associated with growing proportion of TEGDMA. First, the viscosity of the resin mixture decreased, allowing for greater mobility of the reacting species, second, the concentration of functional groups in the reacting system increased due to the incorporation of the monomer with lower molecular weight, and third, reactivity of pendant functional groups increased due to the higher flexibility of diluent monomer backbone. Thus, the propagation reaction becomes restricted by diffusion in the later stages of the reaction and the  $R_{p, \max}$  and vitrification of the emerging network is shifted to the higher conversions (Table 7, Figure 10). The limiting degree of conversion was affected by dilution by the same manner, since the more flexible reacting species with lower molecular volume are able to react further by the segmental diffusion, even after the diffusion-controlled mechanism of propagation prevails. In relation to this assumption, the reports concerning the compositional drift occurrence during copolymerization of base and diluent monomers were

identified in the literature [11,59]. The analysis of leachable components proved that the composition of extracts was not proportional to the composition of initial mixture and that the contribution of low-viscous diluent increases with increasing conversion.

It is obvious, that  $R_{p, \max}$  increased in the case of all copolymerized systems when compared with neat monomers (Figure 10). As it was reported by Dickens *et al.* [14], the initial viscosity influences the reactivity up to the rate where auto-acceleration stops. The reactivity is optimal within the range of viscosities when significant monomer diffusion is allowed on one side, and the segmental movements of macroradicals are restricted due to the gelation on the other. The highest polymerization rate was identified in the case of equimolar mixture of base and diluent monomer, suggesting that in this case, the viscosity was optimal to reach the highest reactivity under the given conditions (i.e. temperature, initiator concentration, light intensity). At lower concentration of diluent monomer, diffusivity of monomers becomes restricted earlier on the conversion scale. In Bis-GMA based resin formulations, this effect is amplified due to the strong hydrogen bonding interactions. In this case, two ether linkages and two methacrylate ester carbonyl groups in TEGDMA can act as the hydrogen bond acceptors. Intermolecular hydrogen bonding between Bis-GMA and TEGDMA can cumulatively enhance the viscosity effects, allowing rapid onset of auto-acceleration [13,60]. Another effect of copolymerization may be the suppression of cyclization reactions. In agreement with kinetic gelation models [38,54], the pendant functional groups become sterically hindered earlier on the conversion scale if the network with increased proportion of effective crosslinks is formed. Indeed, bimodal reaction rate profile was identified only when TEGDMA monomer was in molar excess. Regarding this resin formulation, both lower initial resin viscosity and greater tendency towards primary cyclization, delay the mobility limitation threshold associated with diffusion-controlled mode of termination (i.e. gelation), that allows effective auto-acceleration.

Furthermore, corresponding molar mixtures including ethoxylated analogue of Bis-GMA were studied in order to describe the differences in their reactivity associated with lacking hydrogen bonding sites. As it was discussed above, the extremely high viscosity of Bis-GMA requires the addition of substantial amount of diluent monomer in order to optimize the reactivity. The logarithmic scale of viscosity due to the strong intermolecular hydrogen bonding was identified in Bis-GMA based resin mixtures, ranging between 0.1 and 1000 Pa·s, with respect to molar ratio of base and diluent monomer. On the other hand, the viscosity of Bis-EMA based resin mixtures does not increase dramatically with the increasing content of base monomer (0.1–2 Pa·s) [14]. Thus, an aromatic core structure is not the most important aspect contributing to the reaction behavior. However, the 2-hydroxypropyl groups in Bis-GMA compared to ethoxy groups in Bis-EMA are the main factor causing the differences in copolymerization kinetics. This is due to the impact on viscosity of the resin systems and possible interactions between hydrogen bond donor and acceptor sites.

The increase in reactivity in Bis-EMA based systems was accomplished by addition of relatively small amount of TEGDMA. The addition of TEGDMA causes the severe shift of  $R_{p, \max}$  on the conversion scale and increase of limiting degree of conversion (Table 7, Figures 11, 12). These effects are associated with the lacking hydrogen bonding potential. The

segmental diffusion in the polymerizing systems is facilitated and thus, higher degree of conversion is reached at the onset of auto-deceleration. Bimodal reaction rate profile seen in the case of TEGDMA homopolymerization, is also obvious in the copolymerizations with Bis-EMA (Figure 12). As it was discussed above, this is associated with both low initial viscosity and extensive primary cyclization, delaying the effects associated with the mobility restrictions. In TEGDMA rich resin mixtures, the termination occurs initially by translation (chain-length dependent diffusion of macroradicals). In the later stages, auto-acceleration occurs as a result of decreased frequency of bimolecular termination. The ability of the large radicals to diffuse towards each other becomes impaired, and chain radicals become more mobile by reacting through unreacted monomers. This progress of the reaction is related to the bimodality of the reaction rate profile. The evidence that this effect is primarily related to the initial viscosity of the resin system was published by Young and Bowman [45], who studied the effect of polymerization temperature on reaction-diffusion-controlled termination in the case of DEGDMA homopolymerizations. As the temperature and mobility of the reacting species decrease, the termination becomes diffusion-controlled in the earlier stages of the reaction. As demonstrated for the series of TEGDMA containing resin systems (Figure 12), the onset of reaction-diffusion-controlled termination moves closer to Bis-EMA homopolymerization, where this mechanism dominates from the beginning. In other words, while the rate of termination and propagation decrease during the polymerization course, the changes in relative ratios of these rates are the key factors determining the overall reaction rate profile. When the termination becomes diffusion-controlled, a break in the reaction rate profile is identified, indicating the change in the proportionality between propagation and termination reactions. Afterwards, the propagation is still reaction-controlled, until the decrease associated with diffusion-controlled propagation occurs (i.e. auto-deceleration).

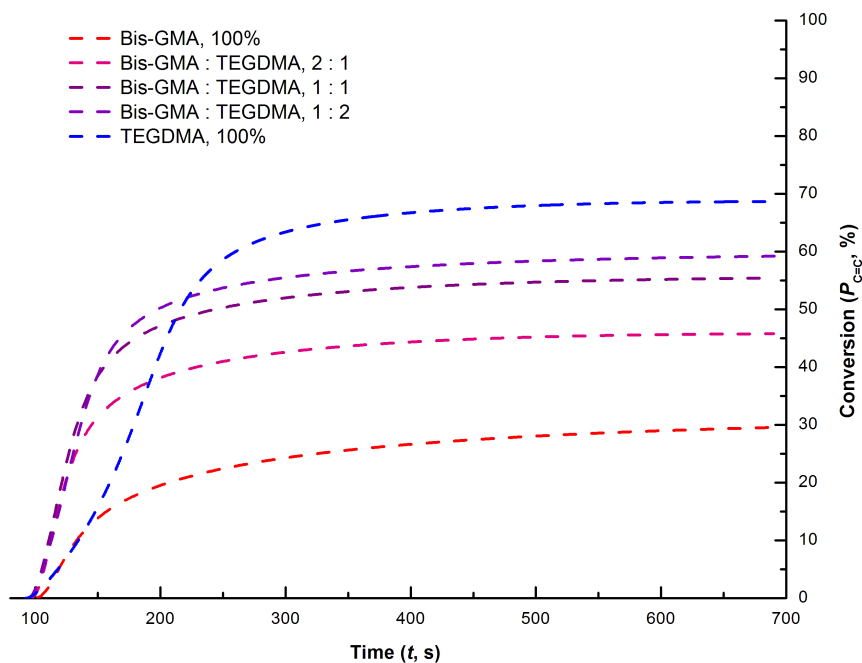


Figure 9: Photo-polymerization kinetic data, degree of double bond conversion as a function of time; Bis-GMA based systems.

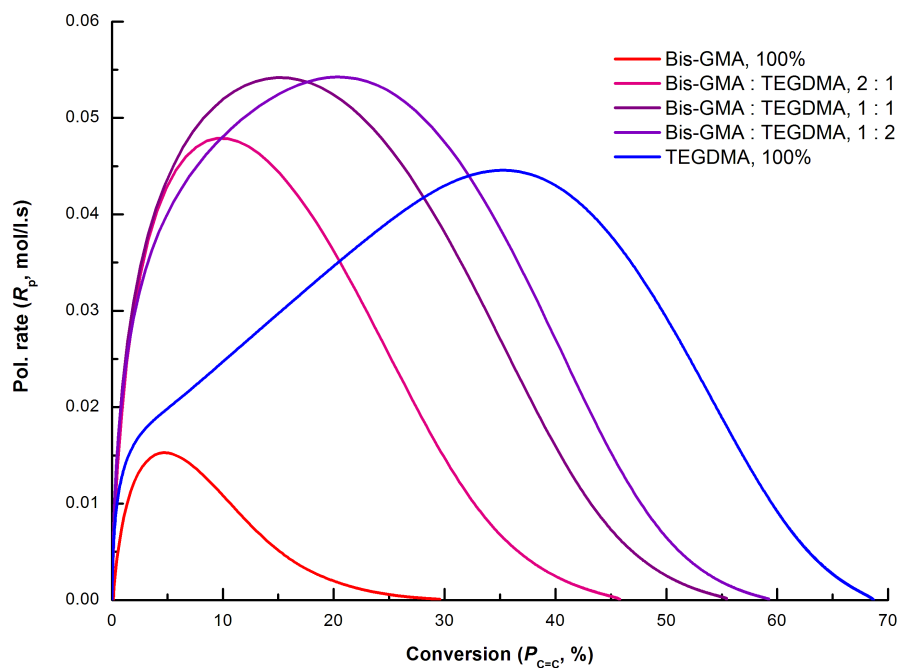


Figure 10: Photo-polymerization kinetic data, reaction rate ( $R_p$ ) normalized by the initial double bond concentration; Bis-GMA based systems.

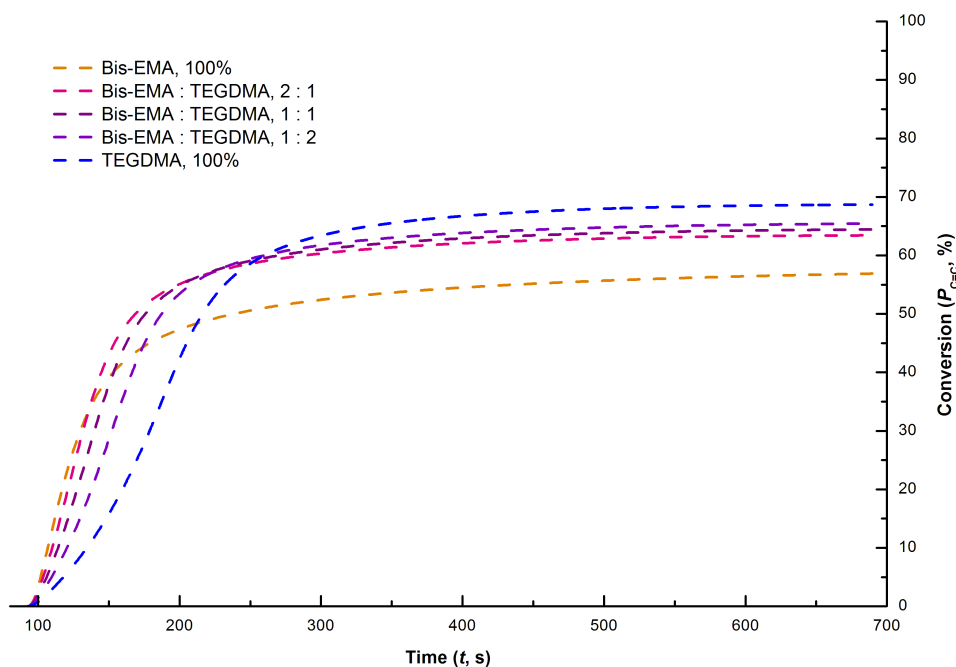


Figure 11: Photo-polymerization kinetic data, degree of double bond conversion as a function of time; Bis-EMA based systems.

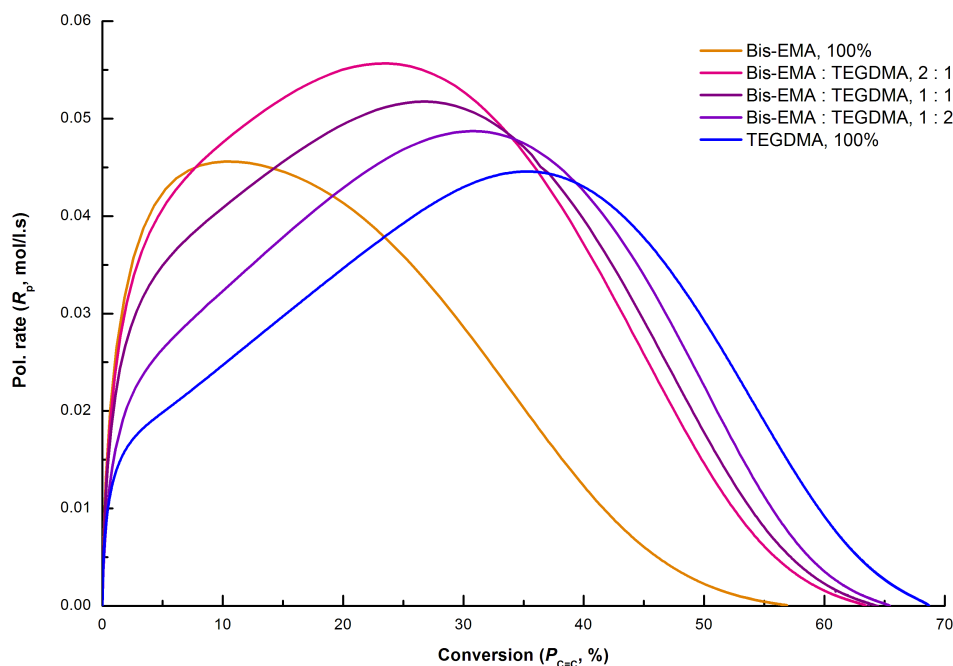


Figure 12: Photo-polymerization kinetic data, reaction rate ( $R_p$ ) normalized by the initial double bond concentration; Bis-EMA based systems.

Table 8 summarizes the threshold parameters of thermal degradation process of copolymers based on different molar ratio of base and diluent monomers.

Table 8: Mean and standard deviation values of temperature where thermal degradation start ( $T_0$ ), and the first ( $T_1$ ) and second ( $T_2$ ) maximum of thermal decomposition and residual mass at 600 °C; Bis-GMA/TEGDMA and Bis-EMA/TEGDMA copolymers.

Designation	$T_0$ [°C]	$T_1$ [°C]	$T_2$ [°C]	Residual mass at 600 °C [%]
Bis-GMA	258.26 (0.72)	/	399.71 (1.22)	14.22 (0.52)
Bis-GMA:TEGDMA, 2:1	243.88 (1.03)	/	400.05 (0.71)	11.06 (0.10)
Bis-GMA:TEGDMA, 1:1	239.30 (2.01)	333.63 (1.30)	401.07 (1.14)	8.73 (0.17)
Bis-GMA:TEGDMA, 1:2	234.35 (1.88)	315.58 (0.91)	399.27 (1.25)	6.75 (0.14)
Bis-EMA	238.97 (1.23)	/	418.71 (0.34)	0.94 (0.13)
Bis-EMA:TEGDMA, 2:1	238.11 (2.20)	341.93 (0.89)	421.30 (1.41)	0.60 (0.29)
Bis-EMA:TEGDMA, 1:1	234.97 (1.73)	339.64 (1.68)	422.10 (1.35)	0.55 (0.12)
Bis-EMA:TEGDMA, 1:2	232.34 (1.54)	330.82 (2.18)	421.37 (1.52)	0.75 (0.13)
TEGDMA	212.37 (2.89)	300.68 (0.46)	379.12 (0.99)	0.46 (0.45)

In case of both Bis-GMA and Bis-EMA based copolymers, with higher content of TEGDMA in the network structure of the copolymer, the temperature of the onset of weight loss ( $T_0$ ) decreases (Figures 13, 15). This suggests that the degree of effective crosslinking in the network structure decreases along with decreasing concentration of the base monomers which are not prone to the primary cyclization reactions. Temperature of the highest degradation rate ( $T_1$ ) of the first phase fluctuates in TEGDMA containing mixtures. The height of dTGA curve decreases and  $T_1$  increases along with increasing content of base monomers (Figures 14, 16). This may be the evidence that the origination of structural inhomogeneities is partially suppressed thanks to the incorporation of base monomers with rigid monomer backbone into the network structure. Based on that assumption, the key parameter affecting the thermal stability of the networks at temperatures above 250 ° C is the degree of effective crosslinking, not the limiting vinyl conversion. The temperature ( $T_2$ ) giving the highest degradation rate in the final phase was constant regardless of the molar concentration of the base and diluent monomers and limiting conversion. Since the height of the dTGA curve implies the quantitative portion of the network with certain structural parameters, it can be concluded that with the growing proportion of rigid base monomer in the comonomer formulation, also the density of effective crosslinks increases and resulting structure appears to be homogeneous. On the other hand, if the proportion of flexible diluent monomer increases, the heterogeneous character of the network becomes more pronounced. The origin of structural heterogeneity was discussed above and interpreted by varying pendant functional groups reactivity and formation of domains with varying extent of effective crosslinking. The kinetics of thermal decomposition of copolymerized networks was also studied by Achilias *et al.* [58] and Rigoli *et al.* [61], reaching the similar conclusions in terms of complexity of thermal decomposition process. The process was characterized by performing isoconversional kinetic analysis. Variations in activation energy attributed to distinct degradation steps were interpreted in the similar way, i.e. by the differences in the structure and the existence of inhomogeneities associated with the kinetic behavior of individual monomer species during copolymerization.

The final point to be discussed are the differences arising from the specific structural features of Bis-GMA and Bis-EMA base monomers. Copolymer Bis-GMA 2:1 follows a behavior of pure Bis-GMA, whereas in the case of the same composition of Bis-EMA based copolymer, a shoulder on dTGA curve appears clearly. This may be the evidence that the primary cyclization reactions are suppressed due to the intermolecular pre-association with Bis-GMA monomer, which is in molar excess. In agreement with Lee *et al.* [60], the presence of hydroxyl groups can lead to formation of multimeric aggregated species thanks to the possible hydrogen bonding interactions between hydroxyl groups, carbonyl and ether functionalities. As the concentration of TEGDMA increases, greater tendency towards origination of inhomogeneities is observed due to greater likelihood of cyclization. The substitution of glycerolate-based side chain for 3 ethoxylated units leads to greater likelihood of primary cyclization reactions, even when the base monomer is in molar excess. This is due to the absence of the hydrogen bond donor functionalities and greater flexibility of Bis-EMA side chains. On the other hand, the temperature giving the highest rate of thermal decomposition in the second step ( $T_2$ ) is higher in the case of Bis-EMA including copolymers. As it was already mentioned above, this is due to a higher degree of covalent crosslinking, which is allowed

thanks to the lower initial viscosity of the resin mixture and the fact, that non-covalent interactions associated with the hydrogen bonds are disrupted by increase of the temperature.

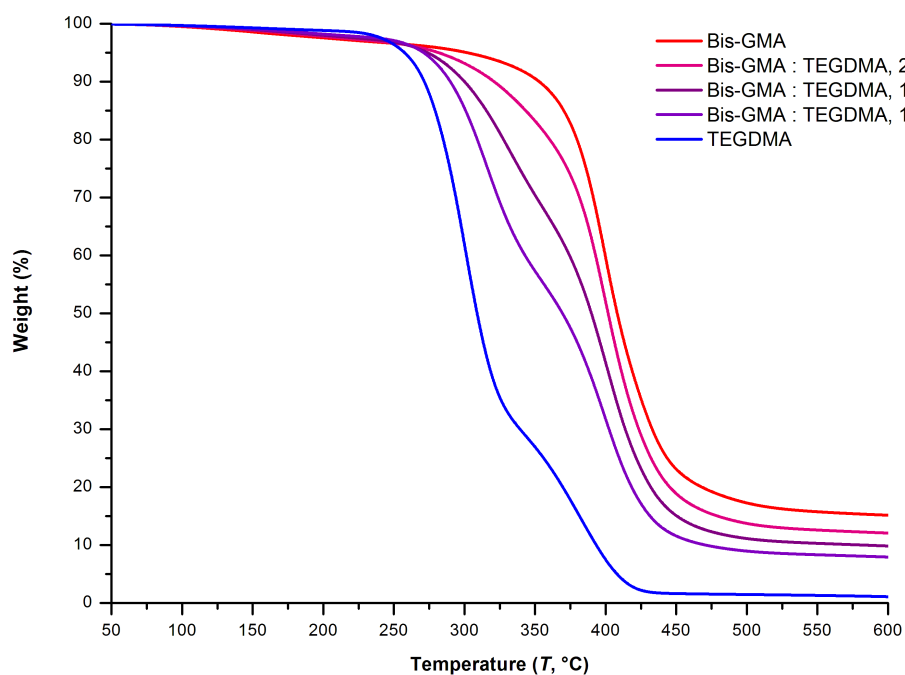


Figure 13: TGA scans, mass loss vs. temperature; Bis-GMA based systems.

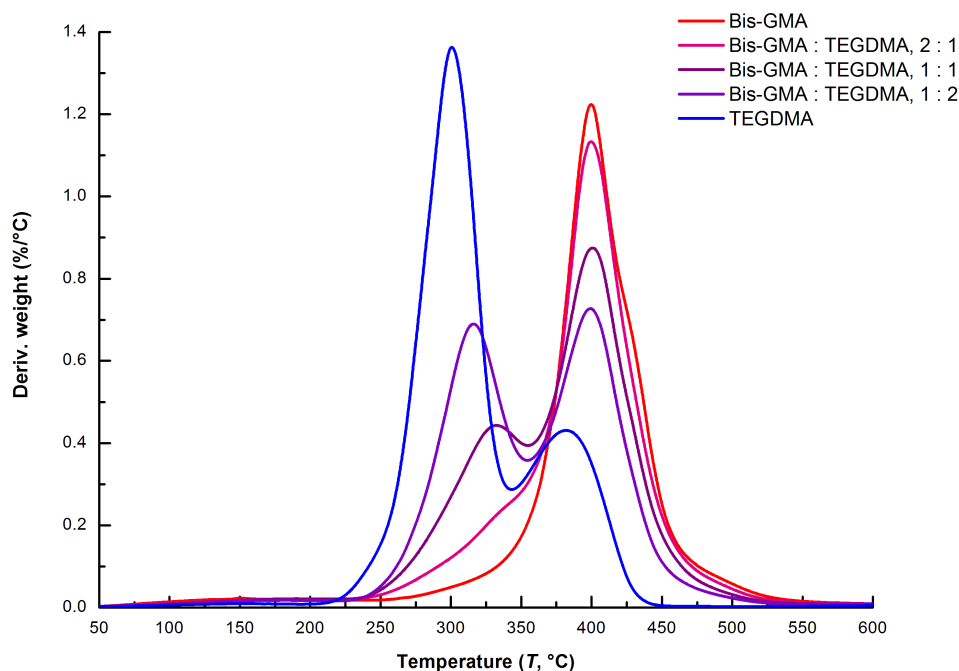


Figure 14: Derivative curves, mass loss vs. temperature; Bis-GMA based systems.

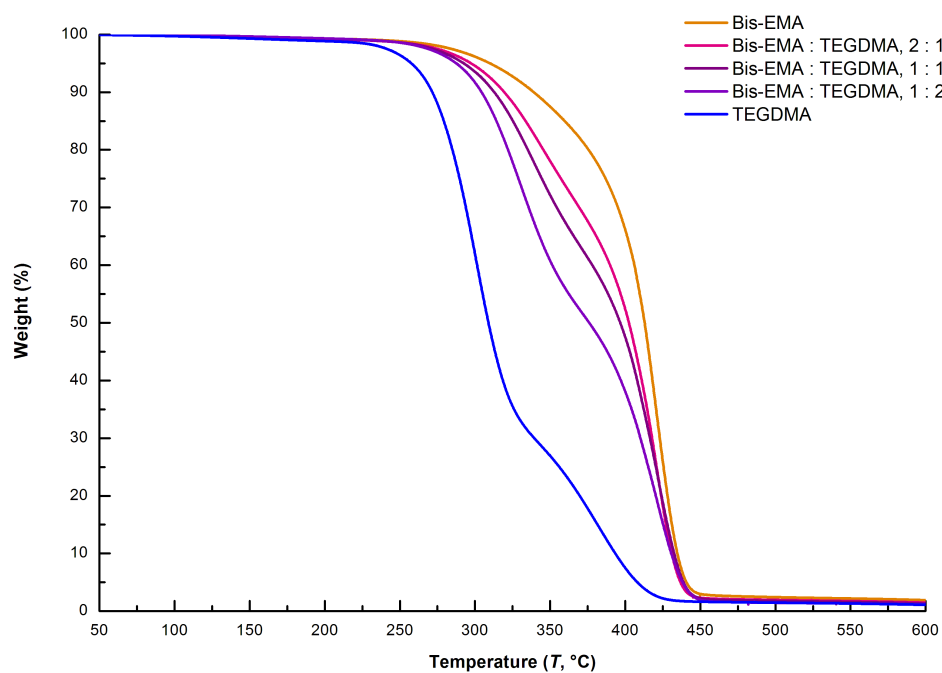


Figure 15: TGA scans, mass loss vs. temperature; Bis-EMA based systems.

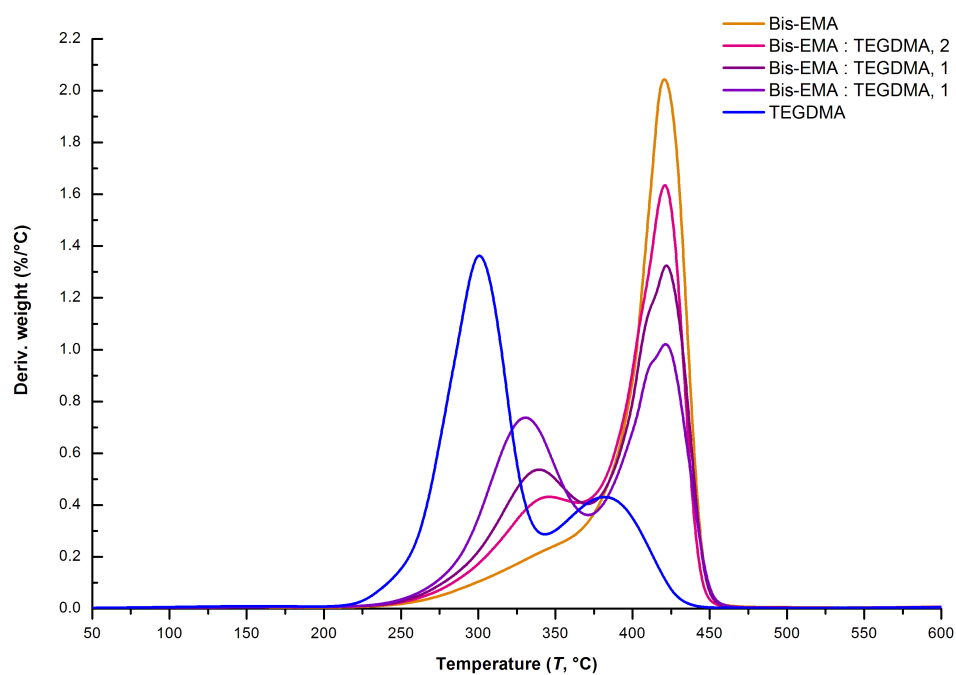


Figure 16: Derivative curves, mass loss vs. temperature; Bis-EMA based systems.

## 5.2 Viscoelastic behavior of dimethacrylate networks

Dynamic-mechanical thermal analysis was used for further structural characterization of homo- and copolymerized dimethacrylate networks. For the purpose of the analysis, conventional photo-initiation system was replaced by organic peroxide, which undergoes homolytic cleavage when exposed to elevated temperatures. Conventional photo-initiator causes complications in the interpretation of the viscoelastic behavior because network structure continues to develop when the temperature is increased above the  $T_g$ . When heated above  $T_g$ , remaining functional groups, residual monomers and unreacted pendant groups with excess free volume regain enough mobility to react further [62]. The temperature range of the curing protocol was chosen to exceed the expected  $T_g$  of dimethacrylate networks during the post-curing period. Experimental observations and theoretical predictions support the hypothesis of close correlation between the cure kinetics of thermally-cured and photo-cured dimethacrylate networks [63]. The increased curing temperature resulted in much higher limiting degree of double bond conversion when compared with photo-cured resin systems, as determined by FTIR analysis (Tables 9 and 10).

To study the complex relation between viscoelastic response and structural parameters of dimethacrylate (co)polymerized networks, complex modulus and damping behavior were recorded under bending load applied at 1 Hz frequency within the temperature range 40–250 °C, i.e. up to and beyond glass transition temperature. The upper temperature is limited by the onset of thermal degradation process.

The course of the storage modulus ( $E'$ ) and loss tangent in the given temperature range are indicative of specific structural features of dimethacrylate networks including effective crosslink density, diverse distribution of micro-environments related to structural heterogeneity, degree of double bonds conversion etc. The storage modulus undergoes a change from the stiff glassy state ( $\sim 2.0$ – $4.0$  GPa) to a rubbery state ( $\sim 0.5$ – $0.7$  GPa). This change is obvious for all characterized dimethacrylate systems, although from the damping behavior (i.e. the width of the loss tangent curve, Figures 17–22) it is clear that the change from the glassy to the rubbery state spreads over a wide range of temperatures. A wide distribution of relaxation times implies a high degree of structural heterogeneity of the networks, consisting of primary chains, effective crosslinks and primary cycles, pendant side chains bearing unreacted functional groups, regions with varying crosslink density etc. Therefore, the glass transition temperature (Tables 9, 10) should not be considered as the specific point at which the whole polymer undergoes glass transition. However, on the comparative basis, the peak of the tangent delta is taken as the glass transition temperature ( $T_g$ ) of the networks. Another important feature that enables to distinguish between the degree of effective crosslinking is the value of the storage modulus in the rubbery region, associated with the concentration of elastically active strands. However, due to the non-Gaussian distribution of chains in highly crosslinked networks and the structural differences between monomer species, the theory of rubber elasticity allowing for calculation of crosslinking density cannot be used [64,65]. The theory, assuming the Gaussian distribution of chains, is limited to the calculations of covalent crosslink density of the networks, where the concentration of crosslinking agent is low, and where there are at least 25 repeating units

between two crosslinks. Due to the aforementioned context, the value of the storage modulus in the rubbery region is used as the measure of crosslink density on the qualitative bases.

### 5.2.1 Homopolymers

The evolution of storage modulus and loss tangent obtained by performing the temperature scans on various homopolymers based on the structurally distinct monomer species (Figures 17, 18), shows considerable differences related to their viscoelastic behavior. As it was extensively discussed in chapter 5.1, the specific structural features of monomers determine the complexity of network-formation kinetics and the resulting supramolecular structure, which is reflected in the viscoelastic response of the networks. Table 9 summarizes the key viscoelastic parameters and limiting degree of conversion of the studied homopolymers.

*Table 9: Mean and standard deviation values of the storage modulus at 40 °C ( $E'$ ) and at the point of glass transition ( $E'_{rubbery}$ ), glass transition temperature ( $T_g$ ) and limiting degree of double bonds conversion ( $P_{C=C}$ ) as determined by FTIR; neat monomers.*

Designation	$E'$ [GPa], 40 °C	$E'_{rubbery}$ [GPa]	$T_g$ [°C]	$P_{C=C}$ [%], FTIR
Bis-GMA	3.85 (0.38)	0.70 (0.08)	178.27 (0.03)	64.32 (2.14)
Bis-EMA	3.51 (0.30)	0.54 (0.06)	154.13 (0.07)	76.43 (1.87)
UDMA	3.25 (0.47)	0.38 (0.04)	151.94 (0.04)	78.92 (3.11)
TEGDMA	1.98 (0.25)	0.54 (0.07)	114.62 (0.02)	89.32 (3.50)

At 40° C, the networks are in the glassy state and the value of the storage modulus is related to the network stiffness, which is highest in the case of Bis-GMA homopolymer regardless the lowest limiting degree of double bonds conversion. This is due to the rigid aromatic character of the Bis-GMA monomer and the presence of two pendant hydroxyl groups providing the additional reinforcement by the strong hydrogen bonding interactions. A slightly lower value of storage modulus of Bis-EMA is given by the lacking hydrogen bonding functionalities, which is partially compensated by a higher achievable limiting degree of conversion when compared with Bis-GMA. UDMA and TEGDMA contain aliphatic spacer group, however, UDMA reaches higher values of storage modulus due to the urethane groups, forming hydrogen bonds [13,60]. Also, higher degree of effective crosslinking is expected in the UDMA based networks. This is related to the larger end-to-end distance, lowering the probability of primary cyclization [38,66], and to the labile hydrogen abstractions from  $-NH-$  groups, favoring chain transfer reactions. Thus, the network is more rigid, considering that there are more crosslinking sites than those based on pendant double bonds [18]. In the case of TEGDMA homopolymer, high degree of primary cyclization does not contribute to the overall mechanical stability of the network.

As the temperature and mobility of the polymer chain increases, steeper decrease of storage modulus occurs in the case of homopolymer systems based on flexible monomers

(i.e. UDMA and TEGDMA) and in the system with lacking hydrogen bonding functionalities. Presence of hydrogen bonds delays the point, where the major portion of the network undergoes the transition to the rubbery state by tightening the network structure. Thermal stability of hydrogen bonding interactions was studied by Kammer *et al.* [67] and later by Morita [68] on Bis-GMA and HEMA polymers, using temperature dependent FTIR and FT-Raman spectroscopy. Even if Bis-GMA polymer is thermally cured up to the degree of conversion of nearly 70 %, only the vibrations of hydroxyl groups, associated with either hydrogen bonding between two hydroxyl groups or between hydroxyl and carbonyl groups are observable [67]. In the case of HEMA homopolymer, it was found that with increasing temperature, the nature of hydrogen bonding interactions slightly changes. The dissociation of hydrogen bonding between hydroxyl groups occurs on one side, whereas in contrast, the association between hydroxyl groups and carbonyl groups occurs on the other [68]. However, this shift is primarily associated with the glass transition temperature of the linear polymer, when the dynamic movements of the whole chain become possible. The hydrogen bond distribution therefore reflects the dynamic nature of the whole system, not only the local dynamics of proton transfer, as it was stated by Li and Brisson [69], who studied the thermal stability of hydrogen bonds in methacrylate copolymers above and below the glass transition temperature within the temperature range of 20–200 °C. As it reported, due to the increased mobility of chains, the number of hydrogen bonding carbonyls decreases above glass transition. When compared with room temperature, it was quantified that about 0.5–3.5 % hydrogen bonds are broken at  $T_g + 30$  °C, depending on the methacrylate comonomer composition.

In the case of Bis-GMA, the expected decrease of hydrogen bonding interactions should be below the decrease quantified in the case of linear methacrylate copolymers. This is due to the presence of covalent crosslinking, affecting the dynamics of chains (mobility becomes increasingly restricted). Thus, as described by van't Hoff relationship, it can be expected, that a small number of hydrogen bonds can be broken or the nature can be slightly changed above  $T_g$ . However, since the  $T_g$  and the value of storage modulus in the rubbery plateau are highest in the case of Bis-GMA homopolymer, despite the lowest limiting degree of conversion (Table 9, Figures 17, 18), it is clear that the physical crosslinks based on hydrogen bonding interactions serves as an effective reinforcement of the network structure in both glassy and rubbery state. As expected, due to the non-Gaussian distribution of chains, the course of the storage modulus in rubbery plateau do not correspond to the concentration of functional groups in the resin mixture (Table 1). Lower values of  $T_g$  and the course of the storage modulus in rubbery plateau are given either by lacking hydrogen bonding functionalities (Bis-EMA), or by aliphatic character of the monomer backbone and the potential for primary cyclization (UDMA and TEGDMA). The different degree of effective crosslinking between UDMA and TEGDMA is given by the different concentration of functional groups and the fact, that the hydrogen bonding interactions associated with the urethane functionalities are weak [13]. A severe disruption of the hydrogen bonding potential is expected to occur above  $T_g$  due to the flexible character of the network.

Besides the measuring of storage modulus and  $T_g$ , the valuable insight into the morphology of the networks is related to the height and breadth of the tangent delta peak (Figure 18),

providing a measure of the range of mobilities existing in the network structure. The height of the transition peak is related to the number of kinetic units contributing to the transition, whereas the breadth depends on the distribution of environments where these units are located [64,70,71]. In other words, these characteristics are directly related to the degree of structural heterogeneity given by the width of the distribution of relaxation times. The heterogeneous character of the networks is attributed to the complexity of parameters that affects polymerization kinetics, including diffusion limitations, physical interactions, and the behavior of pendant functional groups in the vicinity of radical site.

In case of Bis-GMA, the broadness of transition region is related to the low limiting degree of double bonds conversion (i.e. higher concentration of chain ends, pendant side chains or unreacted monomers), and physical crosslinking that may be broken or its character may be slightly changed within the temperature range. Relatively narrower transition regions of Bis-EMA and UDMA are given mainly by the higher degree of double bonds conversion (Table 9). In the case of UDMA, lower extent of primary cyclization is expected to occur when compared with TEGDMA due to the greater molecular weight [35,38,54,66]. Moreover, the effective crosslinking is promoted due to the chain transfer reactions [18,33]. Very wide distribution of relaxation times is apparent from the course of loss tangent in the case of TEGDMA homopolymer, despite the highest degree of conversion. This confirms the idea of spatial heterogeneity associated with the primary cyclization, and coexistence of structurally distinct domains in the network structure. Highly crosslinked microgel regions require more energy to undergo the transition to the rubbery state, whereas the loosely crosslinked regions and pendant side chains are more mobile. Thus, some portions of the network may remain in the rubbery state, deteriorating mechanical properties of the polymer.

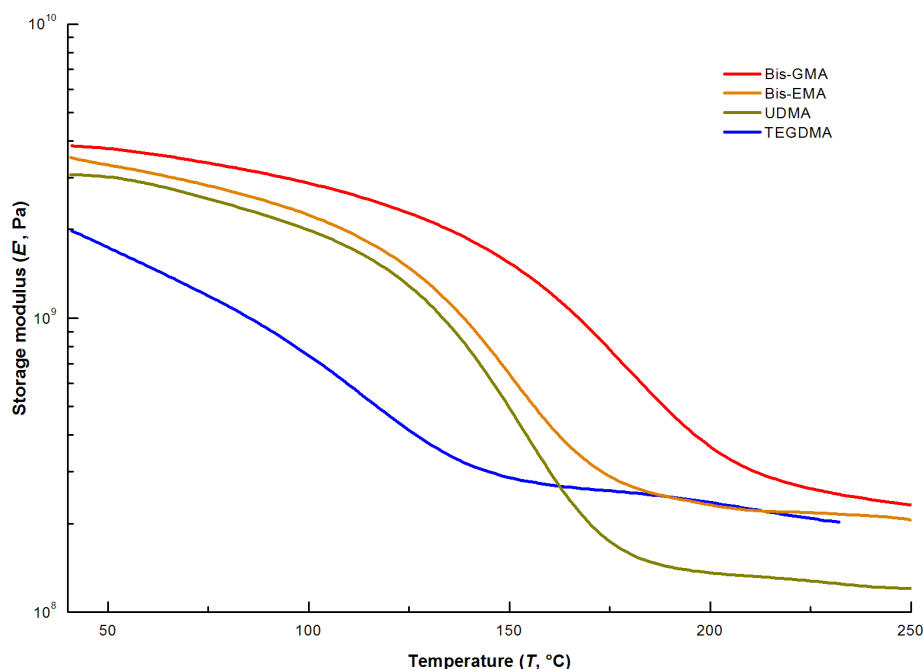


Figure 17: Evolution of the storage modulus as a function of temperature; neat monomers.

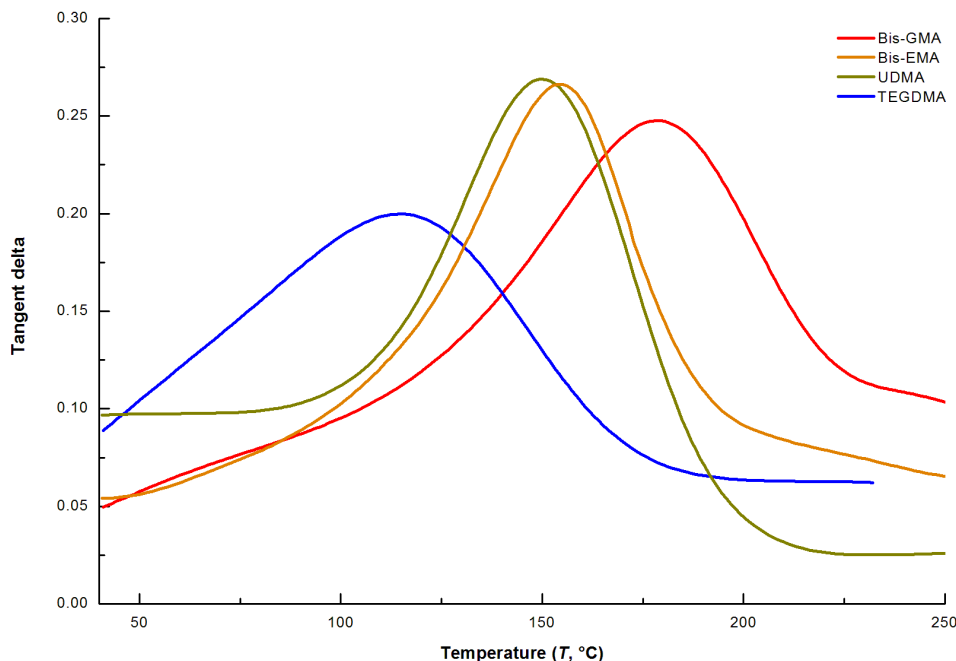


Figure 18: Tangent delta curves as a function of temperature; neat monomers.

### 5.2.2 Copolymers

Evolution of the storage modulus and loss tangent captured over the range of temperature of the systems based on Bis-GMA or Bis-EMA base monomers copolymerized with TEGDMA diluent monomer in different molar ratios are shown on Figures 19–22. Table 10 summarizes the key viscoelastic parameters and limiting degree of double bonds conversion of the studied copolymers. In general, with increasing content of diluent monomer, the storage modulus in the glassy region and the glass transition temperature decrease. Also, single glass transition temperature of the copolymerized systems shows that the polymerization process is random in nature, however, the progress of curing reaction is inhomogeneous due to its kinetic complexity.

The decrease of the storage modulus is given by the increasing proportion of the flexible monomer, which leads to the decrease of network stiffness despite the fact, that the limiting degree of double bonds conversion considerably increase along with increasing proportion of diluent monomer (Figures 19, 21). Thus, it is clear that the decrease in storage modulus and  $T_g$  is not the effect of residual unsaturations, but it is rather associated with the flexibility of the network and effectivity of crosslinking, which may be deteriorated by the occurrence of primary cycles in the network structure. Also, increased range of mobilities coexisting within the network is manifested by broadening of the relaxation times spectra with increasing concentration of diluent monomer (Figures 20, 22). When compared with homopolymers, this is attributed primarily to the varying mobility of the pendant side chains, flexibility of chains between crosslinks, occurrence and the extent of primary cyclization reactions in the Bis-GMA based copolymers and also the variations in the character of physical interactions. The potential range of hydrogen bonding interactions in the copolymerized Bis-GMA/TEGDMA

networks is increased due to the incorporation of electronegative ether donor functionalities in the backbone of TEGDMA [13].

*Table 10: Mean and standard deviation values of the storage modulus at 40 °C ( $E'$ ) and at the point of glass transition ( $E'_{\text{rubbery}}$ ), glass transition temperature ( $T_g$ ) and limiting degree of double bonds conversion ( $P_{C=C}$ ) as determined by FTIR; Bis-GMA/TEGDMA and Bis-EMA/TEGDMA copolymers.*

Designation	$E'$ [GPa], 40 °C	$E'_{\text{rubbery}}$ [GPa], rubbery	$T_g$ [°C]	$P_{C=C}$ [%], FTIR
Bis-GMA	3.85 (0.38)	0.70 (0.08)	178.27 (0.03)	64.32 (2.14)
Bis-GMA:TEGDMA, 2:1	3.47 (0.19)	0.69 (0.06)	172.77 (0.02)	75.02 (2.65)
Bis-GMA:TEGDMA, 1:1	2.93 (0.18)	0.67 (0.08)	166.15 (0.02)	78.23 (1.86)
Bis-GMA:TEGDMA, 1:2	2.84 (0.21)	0.75 (0.05)	167.28 (0.03)	80.42 (1.70)
Bis-EMA	3.51 (0.30)	0.54 (0.06)	154.13 (0.07)	76.43 (1.87)
Bis-EMA:TEGDMA, 2:1	3.33 (0.27)	0.53 (0.08)	150.83 (0.05)	81.72 (1.35)
Bis-EMA:TEGDMA, 1:1	3.07 (0.22)	0.53 (0.08)	146.49 (0.04)	83.27 (1.69)
Bis-EMA:TEGDMA, 1:2	2.90 (0.19)	0.51 (0.05)	138.80 (0.05)	85.13 (1.80)
TEGDMA	1.98 (0.25)	0.54 (0.07)	114.62 (0.02)	89.32 (3.50)

As it was already suggested, the key difference related to the viscoelastic behavior between Bis-GMA and Bis-EMA copolymers is the presence or absence of hydrogen bond donor functionalities. Thus, Bis-GMA based copolymers reach considerably higher  $T_g$  (Table 10), since the hydrogen bonding interactions tightens the network structure. This is also reflected in the course of the storage modulus in the rubbery plateau, indicating the contribution of physical interactions to the overall level of crosslink density. The decrease of extent of primary cyclization reactions of TEGDMA in the copolymerized systems with rigid base monomers is expected in relation to reduced accessibility of the pendant functional groups to the radical site. This is due to the steric hinderance effects in the network structure which is developing with considerable proportion of effective crosslinking. Thus, even if the diluent monomer is in molar excess, there is a significant increase in the storage modulus and  $T_g$ . This increase is more pronounced in the Bis-GMA based systems due to the pre-association between Bis-GMA and TEGDMA monomer species and pendant side chains via intermolecular hydrogen bonding [13]. On the contrary, in the backbone of Bis-EMA monomer, glycerolate-based side chains between methacrylate groups and aromatic core are substituted for flexible ethoxylated units, lacking hydrogen bond donor functionalities. This leads to higher flexibility of the network and greater likelihood of the primary cyclization reactions, resulting in the lower values of the storage modulus in the glassy state as well as in the rubbery plateau, when compared with Bis-GMA based systems.

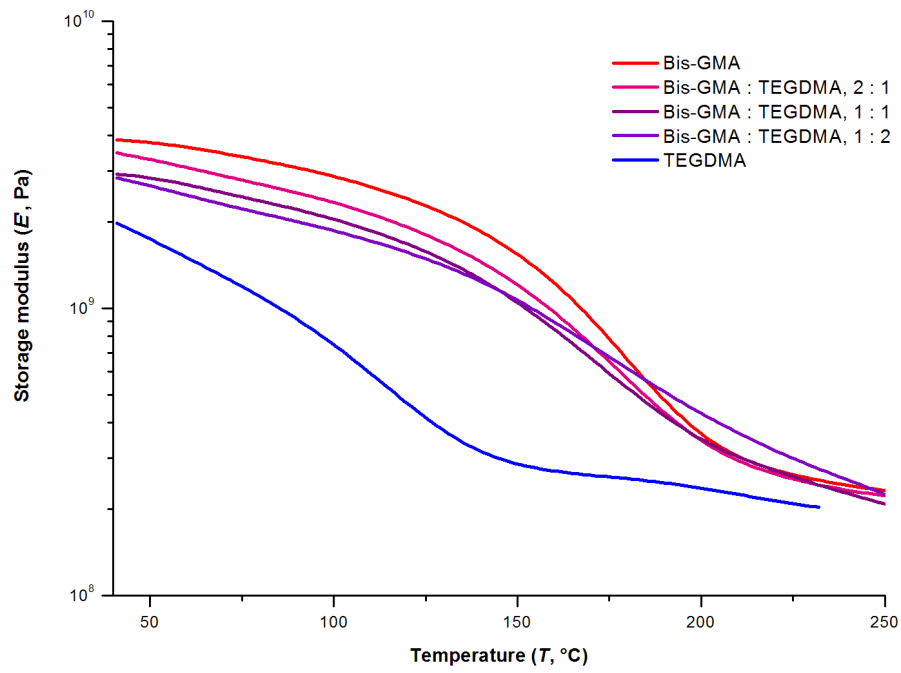


Figure 19: Evolution of the storage modulus as a function of temperature; Bis-GMA based systems.

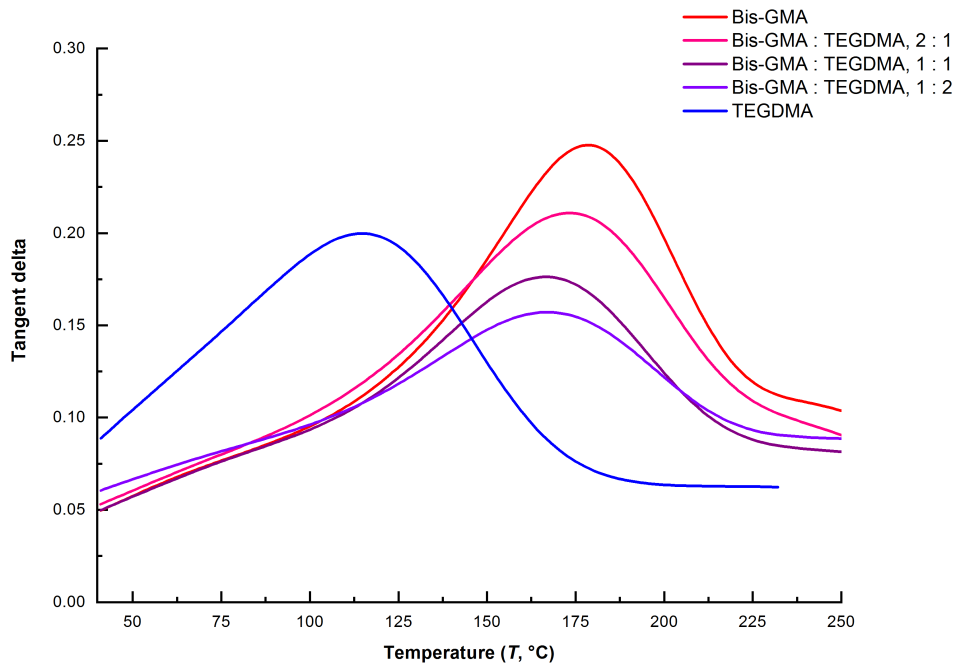


Figure 20: Tangent delta curves as a function of temperature; Bis-GMA based systems.

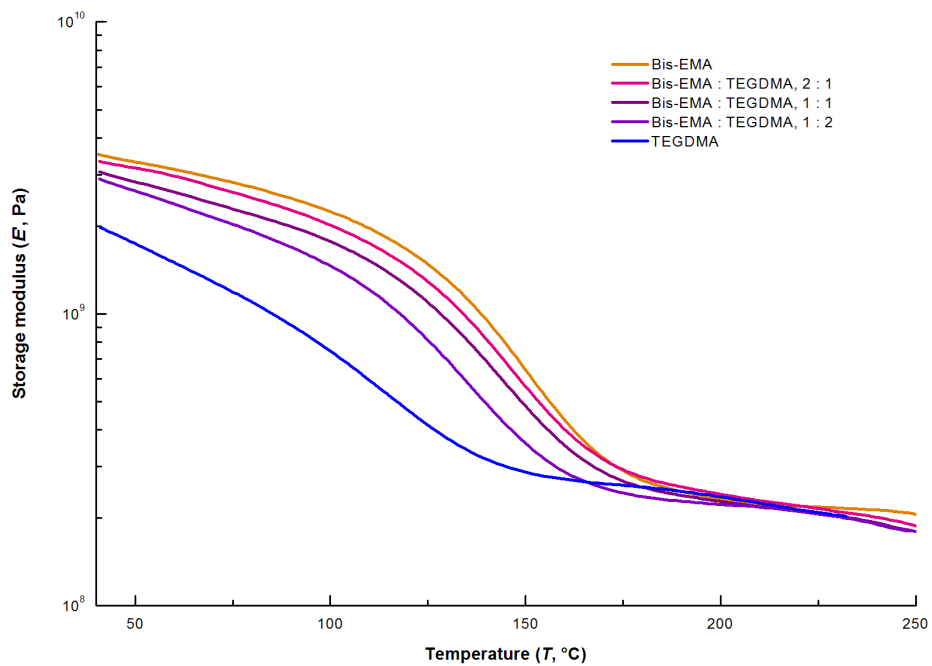


Figure 21: Evolution of the storage modulus as a function of temperature; Bis-EMA based systems.

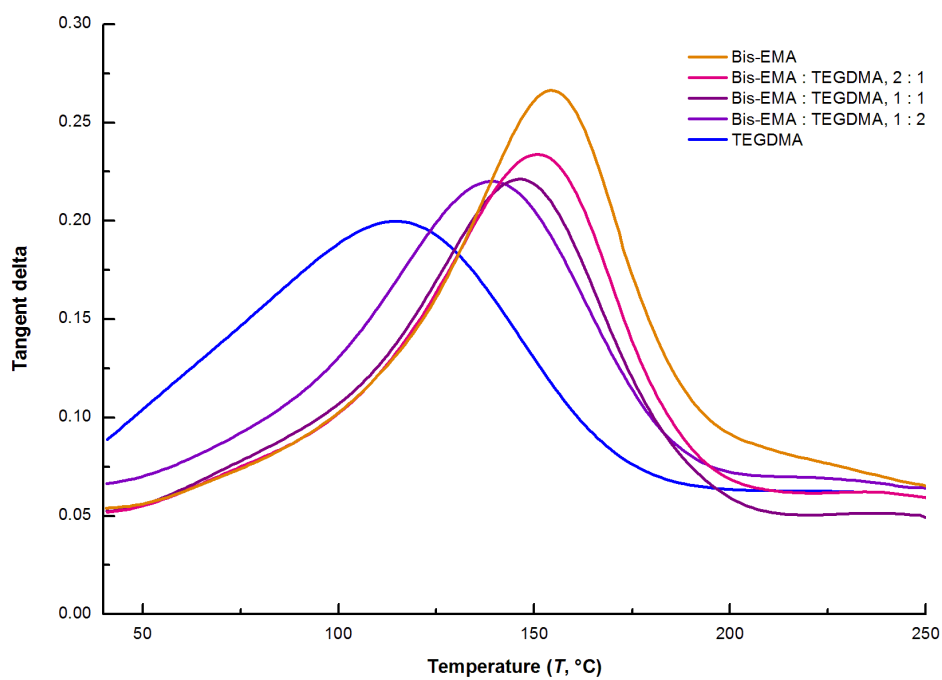


Figure 22: Tangent delta curves as a function of temperature; Bis-EMA based systems.

## 6 CONCLUSION

In this work, the inter-relationship between the structural parameters of dimethacrylate monomers, evolution mechanisms of the network structures and resulting morphology were investigated. Furthermore, viscoelastic parameters of thermally cured networks were determined. Within the scope of this thesis, the resin systems consisting of following monomer species were studied: Bis-GMA, its non-hydroxylated alternative, Bis-EMA, UDMA and PEGDMA with varying molecular weight. In the comonomer resin formulations consisting of base and diluent monomers, TEGDMA was used as the diluent monomer.

The study of kinetics, including the evolution of functional groups conversion and polymerization rate profile, provided insight into the mechanisms of network morphogenesis. In general, due to the crosslinking nature, dimethacrylate systems exhibit complex reaction kinetics including strong mobility restrictions of kinetic units during the network development. This includes auto-acceleration, auto-deceleration, and varying pendant functional groups reactivity throughout the polymerization process. Incomplete curing reaction and entrapment of radicals are the inevitable result of diffusion-controlled reaction.

Based on the homopolymerization kinetics of the aforementioned monomers, it was found that the rate of polymerization and the degree of conversion are severely limited by the stiff aromatic character of monomer backbone in case of Bis-GMA, Bis-EMA, and high initial viscosity of the resin systems given by the contribution of strong hydrogen bonding interactions (Bis-GMA). On the other hand, rigidity of these monomers decreases the probability of primary cyclization reactions due to the steric hinderance effects, which leads to higher effectivity of crosslinking. Higher reactivity is related primarily to a lower molecular volume, and higher flexibility of aliphatic monomer backbone (UDMA, PEGDMA). However, flexibility of the monomer and proximity of the pendant functional group to the radical site, given by the decreasing molecular weight of monomers, lead to a greater probability of the propagation via primary cyclization, and inhomogeneous course of the network formation. Heterogeneous polymerization is reflected in the morphogenesis characterized by microgel domains formation preceded by extensive cyclization, followed by formation of interconnections among the domains. These results are in good agreement with the numerical models that simulate the kinetics of free radical network polymerization (i.e. kinetic gelation models) and the kinetics of primary cyclization reactions.

A copolymerization kinetics of base (Bis-GMA, Bis-EMA) and diluent monomers (TEGDMA) show intermediate behavior between those of the corresponding pure monomers. The dilution leads to an increased mobility in the polymerizing systems. Hence, the optimal reactivity can be reached by optimizing a molar ratio of the base and diluent monomers under the given conditions. However, despite the higher limiting degree of conversion reached in relation to the dilution effect, the effectivity of crosslinking decreases as the potential for inhomogeneous progress of curing reaction increases along with increasing concentration of TEGDMA. Because the gelation occurs very early on the conversion scale, the phase separation is suppressed despite any thermodynamic instability of the marginally compatible mixture of monomers during copolymerization, and the process is random. The possible

compositional drift is given only by the differences in mobility of the monomer species in the polymerizing systems. Thus, the inhomogeneous curing character is given predominantly by the anomalous behavior of the various kinetic units during the polymerization.

The rate of polymerization given by the concentration of active radicals controls the kinetic chain length at the point of termination. Shorter chains with fewer functional groups do not restrict the mobility in the reacting system as much as longer chains do, allowing for higher rate of segmental diffusion. Hence, the mobility of macroradicals and monomers becomes severely restricted by diffusion slightly later on the conversion scale and the systems reach higher limiting degree of conversion.

Differences in the morphology of cured resins influence the degradation behavior. Bis-GMA and Bis-EMA monomers form a more rigid networks due to their rigid aromatic backbone and higher degree of effective crosslinking, decomposing at higher temperatures when compared with the series of PEGDMA and UDMA. The presence of structural inhomogeneities in the structure of the networks based on the monomers that undergo cyclization reactions to a greater extent is manifested by the appearance of two degradation steps. This is associated with the different thermal stability of the coexisting regions with varying crosslink density.

The progress of the storage modulus vs. temperature, recorded under the bending load applied at given frequency across the glass transition, reflects the network stiffness, effectivity of crosslinking, degree of conversion and the reinforcement of the network structure by physical interactions. In case of copolymers, the occurrence of the single transition temperature confirms that the copolymerization process is random in nature. The stiffness of the monomer backbone, as well as tightening of the structure by the hydrogen bonding interactions, leads to higher values of the storage modulus in a glassy state and higher temperatures of the transition into a rubbery state. Thus, both aforementioned values are the highest for the Bis-GMA homopolymer despite the lowest limiting degree of conversion. The qualitative estimation of the effective crosslink density, given by the progress of the storage modulus in the rubbery plateau, confirms the assumption that the effectivity of crosslinking is not directly related to the initial concentration of double bonds and the degree of conversion, but rather to the reactivity of pendant functional groups. The degree of structural heterogeneity is manifested by the broadness of the relaxation times spectra, providing a measure of the range of mobilities in the network structure.

The results of this work provide the basis for a rational design of crosslinking systems including matrices of dental resin composites. However, further characteristics beyond the scope of this work related to particular application must be taken into the consideration to develop the systems with optimized outcome. Although Bis-GMA monomer was introduced nearly 60 years ago, the results of this work identifies Bis-GMA as an essential component of the resin formulations, because its stiffness as well as the potential for strong intermolecular hydrogen bonding contribute to the formation of durable and more homogeneous polymer networks.

## 7 REFERENCES

- [1] BOWEN, R. L. Dental filling material comprising vinyl-silane treated fused silica and a binder consisting of the reaction product of bisphenol and glycidyl methacrylate [patent]. *US patent*. 3,006,112. 1962.
- [2] BOWEN, R. L. Silica-resin direct filling material and method of preparation [patent]. *US patent*. 3,194,783. 1965.
- [3] PEUTZFELD, A. Resin composites in dentistry: the monomer systems. *European Journal of Oral Sciences*. 1997, 105(2), 97–116.
- [4] STANSBURY, J. W. Dimethacrylate network formation and polymer property evolution as determined by the selection of monomers and curing conditions. *Dental Materials*. 2012, 28(1), 13–22.
- [5] TANTBIJORN, D., C. S. PFEIFER, R. R. BRAGA and A. VERSLUIS. Do low-shrink composites reduce polymerization shrinkage effects? *Journal of Dental Research*. 2011, 90(5), 596–601.
- [6] LEPRINCE, J. G., W. M. PALIN, M. A. HADIS, J. DEVAUX and G. LELOUP. Progress in dimethacrylate-based dental composite technology and curing efficiency. *Dental Materials*. 2013, 29(2), 139–156.
- [7] GONÇALVES, F., Y. KAWANO, C. PFEIFER, J. W. STANSBURY and R. R. BRAGA. Influence of Bis-GMA, TEGDMA and Bis-EMA contents on viscosity, conversion and flexural strength of experimental resins and composites. *European Journal of Oral Sciences*. 2009, 117(4), 442–446.
- [8] PFEIFER, C. S., L. R. SILVA, Y. KAWANO and R. R. BRAGA. Bis-GMA copolymerizations: Influence on conversion, flexural properties, fracture toughness and susceptibility to ethanol degradation of experimental composites. *Dental Materials*. 2009, 25(9), 1146–1141.
- [9] JANCAR, J., W. WANG and A. T. DIBENEDETTO. On the heterogeneous structure of thermally cured bis-GMA/TEGDMA resins. *Journal of Materials Science: Materials in Medicine*. 2000, 11(11), 675–682.
- [10] SHAH, P. K. and J. W. STANSBURY. Conversion dependent evolution of shrinkage, modulus and stress: Filler effects. *Dental Materials* [online]. 2009, 25(5), e29.
- [11] STANSBURY, J. W. and S. H. DICKENS. Network formation and compositional drift during photo-initiated copolymerization of dimethacrylate monomers. *Polymer*. 2001, 42(15), 6363–6369.

- [12] LOVELL, L. G., J. W. STANSBURY, D. C. SYRPES and C. N. BOWMAN Effects of composition and reactivity on the reaction kinetics of dimethacrylate/dimethacrylate co-polymerizations. *Macromolecules*. 1999, 32(12), 3913–3921.
- [13] LEMON, M. T., M. S. JONES and J. W. STANSBURY. Hydrogen bonding interactions in methacrylate monomers and polymers. *Journal of Biomedical Materials Research A*. 2007, 83(3), 734–746.
- [14] DICKENS, S. H., J. W. STANSBURY, K. M. CHOI and C. J. E. FLOYD. Photopolymerization kinetics of methacrylate dental resins. *Macromolecules*. 2003, 36(16), 6043–6053.
- [15] ANSETH, K. S., M. D. GOODNER, M. A. REIL, A. R. KANNURPATTI, S. M. NEWMAN and C. N. BOWMAN. The influence of co-monomer composition on dimethacrylate resin properties for dental composites. *Journal of Dental Research*. 1996, 75(8), 607–1612.
- [16] FONSECA, A. S. Q. S., A. D. L. MOREIRA, P. P. A. C. DE ALBUQUERQUE, L. R. DE MENEZES, C. S. PFEIFER and L. F. J. SCHNEIDER. Effect of monomer type on the C=C degree of conversion, water sorption and solubility, and color stability of model dental composites. *Dental Materials*. 2017, 33(4), 394–401.
- [17] MOSZNER, N. and U. SALZ. New developments of polymeric dental composites. *Progress in Polymer Science*. 2001, 26(4), 535–576.
- [18] SIDERIDOU, I., V. TSERKI and G. PAPANASTASIOU. Effect of chemical structure on degree of conversion in light-cured dimethacrylate-based dental resins. *Biomaterials*. 2002, 23(8), 1819–1829.
- [19] WATTS, D. and N. SILIKAS. *Dental hard tissues and bonding: interfacial phenomena and related properties*. 1<sup>st</sup>. ed. New York, NY: Springer, 2005, 123–154. ISBN 978-3-540-23408-1.
- [20] ANSETH, K. S., C. M. WANG, and C. N. BOWMAN. Reaction behavior and kinetic constants for photo-polymerizations of multi (meth)acrylate monomers. *Polymer*. 1994, 35(15), 3243–3250.
- [21] ANSETH, K. S., L. M. KLINE, T. A. WALKER, K. J. ANDERSON and C. N. BOWMAN. Reaction kinetics and volume relaxation during polymerizations of multi-ethylene glycol dimethacrylates. *Macromolecules*. 1995, 28(7), 2491–2499.
- [22] LEPRINCE, J. G., G. LAMBLIN, J. DEVAUX, M. DEWAELE, M. MESTDAGH, W. M. PALIN, B. GALLEZ and G. LELOUP. Irradiation mode's impact on radical entrapment in photoactive resins. *Journal of Dental Research*. 2010, 89(12), 1494–1498.

- [23] ANSETH, K. S., C. M. WANG and C. N. BOWMAN. Kinetic evidence of reaction diffusion during the polymerization of multi(meth)acrylate monomers. *Macromolecules*. 1994, 27(3), 650–655.
- [24] IKEMURA, K. and T. ENDO. A review of the development of radical photo-polymerization initiators used for designing light-curing dental adhesives and resin composites. *Dental Materials Journal*. 2010, 29(5), 481–501.
- [25] STANSBURY, J. W. Curing dental resins and composites by photo-polymerization. *Journal of Esthetic Dentistry*. 2000, 12(6), 300–308.
- [26] JAKUBIAK, J., X. ALLONAS, J. P. FOUASSIER and J. RABEK. Camphorquinone-amines photo-initiating systems for the initiation of free radical polymerization. *Polymer*. 2003, 44(18), 5219–5226.
- [27] KURDIKAR, D. L. and N. A. PEPPAS. A kinetic model for diffusion-controlled bulk crosslinking photo-polymerizations. *Macromolecules*. 1994, 27(15), 4084–4092.
- [28] COOK, W. D. Photo-polymerization kinetics of dimethacrylates using the camphorquinone/amine initiator system. *Polymer*. 1992, 33(3), 600–609.
- [29] WATTS, D. C. Reaction kinetics and mechanics in photo-polymerized networks. *Dental Materials*. 2005, 21(1), 27–35.
- [30] ANDRZEJEWSKA, E. Photo-polymerization kinetics of multifunctional monomers. *Progress in Polymer Science*. 2001, 26(4), 605–665.
- [31] DECKER, C. and K. MOUSSA. Radical trapping in photo-polymerized acrylic networks. *Journal of Polymer Science*. 1987, 25(2), 739–742.
- [32] ANDRZEJEWSKA, E., E. SOCHA and M. ANDRZEJEWSKI. Crosslinking photocopolymerization of dodecyl methacrylate with oxyethyleneglycol dimethacrylates: Kinetics and reactivity ratios. *Polymer*. 2006, 47(19), 6513–6523.
- [33] SIDERIDOU, I. D., D. S. ACHILIAS and N. C. KOSTIDOU. Copolymerization kinetics of dental dimethacrylate resins initiated by a benzoyl peroxide/amine redox system. *Journal of Applied Polymer Science*. 2008, 109(1), 515–524.
- [34] PODGÓRSKI, M. Structure-property relationship in new photo-cured dimethacrylate-based dental resins. *Dental Materials*. 2012, 28(4), 398–409.
- [35] ELLIOTT, J. E., L. G. LOVELL and C. N. BOWMAN. Primary cyclization in the polymerization of bis-GMA and TEGDMA: a modeling approach to understanding the cure of dental resins. *Dental Materials*. 2001, 17 (3), 221–229.
- [36] DUŠEK, K. Special features of network formation by chain crosslinking copolymerization. *Collection of Czechoslovak Chemical Communications*. 1993, 58(10), 2245–2265.

- [37] BARSZCZEWSKA-RYBAREK, I. M. and M. KRASOWSKA. Fractal analysis of heterogeneous polymer networks formed by photo-polymerization of dental dimethacrylates. *Dental Materials*. 2012, 28(6), 695–702.
- [38] ANSETH, K. S., and C. N. BOWMAN. Kinetic gelation model predictions of cross-linked polymer network microstructure. *Chemical Engineering Science*. 1994, 49(14), 2207–2217.
- [39] ELLIOTT, J. E. and C. N. BOWMAN. Kinetics of primary cyclization reactions in crosslinked polymers: an analytical and numerical approach to heterogeneity in network formation. *Macromolecules*. 1999, 32(25), 8621–8628.
- [40] SIDERIDOU, I. a M. M. KARABELA. Sorption of water, ethanol or ethanol/water solutions by light-cured dental dimethacrylate resins. *Dental Materials*. 2011, 27(10), 1003–1010.
- [41] NAGHASH, H. J., O. OKAY and Y. YAĞCI. Gel formation by chain-crosslinking photopolymerization of methyl methacrylate and ethylene glycol dimethacrylate. *Polymer*. 1997, 38(5), 1187–1196.
- [42] ACHILIAS, D. S. and G. D. VERROS. Modeling of diffusion-controlled reactions in free radical solution and bulk polymerization: Model validation by DSC experiments. *Journal of Applied Polymer Science*. 2010, 116(3), 1842–1856.
- [43] BOWMAN, C. N. and C. J. KLOXIN. Toward an enhanced understanding and implementation of photo-polymerization reactions. *AIChE Journal*. 2008, 54(11), 2775–2795.
- [44] YE, S., N. B. CRAMER and C. N. BOWMAN. Relationship between glass transition temperature and polymerization temperature for cross-linked photopolymers. *Macromolecules*. 2011, 44(3), 490–494.
- [45] YOUNG, J. S. a C. N. BOWMAN. Effect of Polymerization Temperature and Cross-Linker Concentration on Reaction Diffusion Controlled Termination. *Macromolecules*. 1999, 32(19), 6073–6081.
- [46] HOWARD, B., N. D. WILSON, S. M. NEWMAN, C. S. PFEIFER and J. W. STANSBURY. Relationships between conversion, temperature and optical properties during composite photo-polymerization. *Acta Biomaterialia*. 2010, 6(6), 2053–2059.
- [47] ROSENTRITT, M., A. C. SHORTALL and W. M. PALIN. Dynamic monitoring of curing photoactive resins: A methods comparison. *Dental Materials*. 2010, 26(5), 565–570.
- [48] TESHIMA, W., Y. NOMURA, A. IKEDA, T. KAWAHARA, M. OKAZAKI and Y. NAHARA. Thermal degradation of photo-polymerized Bis-GMA/TEGDMA based dental resins. *Polymer Degradation and Stability*. 2004, 84(1), p. 167–172.

- [49] ACHILIAS, D. S., M. M. KARABELA and I. D. SIDERIDOU. Thermal degradation of light-cured dimethacrylate resins: Part I. Isoconversional kinetic analysis. *Thermochimica Acta*. 2008, 472(1–2), 74–83.
- [50] VOVOUDI, E. C., D. S. ACHILIAS and I. D. SIDERIDOU. Dental light-cured nano-composites based on a dimethacrylate matrix: Thermal degradation and isoconversional kinetic analysis in N<sub>2</sub> atmosphere. *Thermochimica Acta*. 2015, 599, 63–72.
- [51] MARTIM, G. C., C. S. PFEIFER and E. M. GIROTTO. Novel urethane-based polymer for dental applications with decreased monomer leaching. *Materials Science and Engineering: C*. 2017, 72(1), 192–201.
- [52] KHATRI, C. A., J. W. STANSBURY, C. R. SCHULTHEISZ and J. M. ANTONUCCI. Synthesis, characterization and evaluation of urethane derivatives of Bis-GMA. *Dental Materials*. 2003, 19(7), 584–588.
- [53] BARSZCZEWSKA-RYBAREK, I. M. Characterization of urethane-dimethacrylate derivatives as alternative monomers for the restorative composite matrix. *Dental Materials*. 2014, 30(12), 1336–1344.
- [54] WEN, M., L. E. SCRIVEN and A. V. MCCORMICK. Kinetic Gelation Modeling: Kinetics of Cross-Linking Polymerization. *Polymer*. 2003, 36(11), 4151–4159.
- [55] PIELICHOWSKI, K. and J. NJUGUNA. *Thermal Degradation of Polymeric Materials*. Shawbury, Shropshire, SY4 4NR, United Kingdom: Smithers Rapra Technology, 2005. ISBN 1-85957-498-X.
- [56] REY, L., J. DUCHET, J. GALY, H. SAUTERAU, D. VOUAGNER and L. CARRION. Structural heterogeneities and mechanical properties of vinyl/dimethacrylate networks synthesized by thermal free radical polymerization. *Polymer*. 2002, 43(16), 4375–4384.
- [57] BARSZCZEWSKA-RYBAREK, I. M. Structure–property relationships in dimethacrylate networks based on Bis-GMA, UDMA and TEGDMA. *Dental Materials*. 2009, 25(9), 1082–1089.
- [58] ACHILIAS, D. S. and I. SIDERIDOU. Thermal degradation and isoconversional kinetic analysis of light-cured dimethacrylate copolymers. *Journal of Thermal Analysis and Calorimetry*. 2010, 99(3), 917–923.
- [59] FLOYD, C. J. E. and S. H. DICKENS. Network structure of Bis-GMA-, and UDMA-based resin systems. *Dental Materials*. 2006, 22(12), 1143–1149.
- [60] LEE, T. Y., T. M. ROPER, E. S. JÖNSSON, C. A. GUYMON and C. E. HOYLE. Influence of Hydrogen Bonding on Photopolymerization Rate of Hydroxyalkyl Acrylates. *Macromolecules*. 2004, 37(10), 3659–3665.

- [61] RIGOLI, I. C., C. C. S. CAVALHEIRO, M. G. NEUMANN and E. T. G. CAVALHEIRO. Thermal Decomposition of Copolymers Used in Dental Resins Formulations Photocured by Ultra Blue IS. *Journal of Applied Polymer Science*. 2007, 105(6), 3295–3330.
- [62] LEE, J. K., J. CHOI, B. LIM, Y. LEE and R. L. SAKAGUCHI. Change of Properties during Storage of a UDMA/TEGDMA Dental Resin. *Journal of Biomedical Materials Research, Part B, Applied Biomaterials*. 2004, 68(2), 216–221.
- [63] C. E. HOYLE and P. S. PAPPAS. Radiation curing: science and technology. 1st ed. New York: Springer Science Business Media, 1992, s. 57-133. Topics in applied chemistry. ISBN 978-1-4899-0714-1.
- [64] YU, Q., M. ZHOU, Y. DING, B. JIANG and S. ZHU. Development of networks in atom transfer radical polymerization of dimethacrylates. *Polymer*. 2007, 48(24), 7058–7064.
- [65] DUŠEK, K. and W. J. M. PRINS. Structure and Elasticity of Non-Crystalline Polymer Networks. *Advances in Polymer Science*. 1969, 6(16), 1–102.
- [66] ELLIOT, J. E., J. W. ANSETH and C. N. BOWMAN. Kinetic modeling of the effect of solvent concentration on primary cyclization during polymerization of multifunctional monomers. *Chemical Engineering Science*. 2001, 56(10), 3173–3184.
- [67] KAMMER, S., K. ALBINSKY, B. SANDNER and S. WARTEWIG. Polymerization of hydroxyalkyl methacrylates characterized by combination of FT-Raman and step-scan FT-i.r. photoacoustic spectroscopy. *Polymer*. 1999, 40(5), 1131–1137.
- [68] MORITA, S. Hydrogen-Bonds Structure in Poly(2-Hydroxyethyl Methacrylate) Studied by Temperature-Dependent Infrared Spectroscopy. *Frontiers in Chemistry*. 2014, 2(10), 1–5.
- [69] LI, D. and J. BRISSON. Hydrogen bonds in poly(methyl methacrylate)- poly(4-vinyl phenol) blends: Quantification near the glass transition temperature. *Polymer*. 1998, 39(4), 801–810.
- [70] LOVELL, L. G., K. A. BERCHTOLD, J. E. ELLIOTT and C. N. BOWMAN. Understanding the kinetics and network formation of dimethacrylate dental resins. *Polymers for Advanced Technologies*. 2001, 12(6), 335–345.
- [71] KALAKKUNNATH, S., D. S. KALIKA, H. LIN and B. D. FREEMAN. Viscoelastic characteristics of UV polymerized poly(ethylene glycol) diacrylate networks with varying extents of crosslinking. *Journal of Polymer science: Part B: Polymer Physics*. 2006, 44(15), 2058–2070.

## LIST OF FIGURES

- Figure 1:** Monomer structure of Bis-GMA base monomer (Bowen monomer).
- Figure 2:** Monomer structures of low-viscous diluent monomers, TEGDMA and HDDMA.
- Figure 3:** Monomer structures of alternative base monomers, UDMA and Bis-EMA
- Figure 4:** Molecular structures of most commonly used photo-initiator system including photosensitizer (camphorquinone) and photo-reducing agent (dimethylamino-ethyl methacrylate).
- Figure 5:** Photo-polymerization kinetic data, degree of double bond conversion as a function of time; neat monomers.
- Figure 6:** Photo-polymerization kinetic data, reaction rate ( $R_p$ ) normalized by the initial double bond concentration; neat monomers.
- Figure 7:** TGA scans, mass loss vs. temperature; of neat monomers.
- Figure 8:** TGA scans, derivative curves, mass loss vs. temperature; neat monomers.
- Figure 9:** Photo-polymerization kinetic data, degree of double bond conversion as a function of time; Bis-GMA based systems.
- Figure 10:** Photo-polymerization kinetic data, reaction rate ( $R_p$ ) normalized by the initial double bond concentration; Bis-GMA based systems.
- Figure 11:** Photo-polymerization kinetic data, degree of double bond conversion as a function of time; Bis-EMA based systems.
- Figure 12:** Photo-polymerization kinetic data, reaction rate ( $R_p$ ) normalized by the initial double bond concentration; Bis-EMA based systems.
- Figure 13:** TGA scans, mass loss vs. temperature; Bis-GMA based systems.
- Figure 14:** Derivative curves, mass loss vs. temperature; Bis-GMA based systems.
- Figure 15:** TGA scans, mass loss vs. temperature; Bis-EMA based systems.
- Figure 16:** Derivative curves, mass loss vs. temperature; Bis-EMA based systems.
- Figure 17:** Evolution of the storage modulus as a function of temperature; neat monomers.
- Figure 18:** Tangent delta curves as a function of temperature; neat monomers.
- Figure 19:** Evolution of the storage modulus as a function of temperature; Bis-GMA based systems.
- Figure 20:** Tangent delta curves as a function of temperature; Bis-GMA based systems.
- Figure 21:** Evolution of the storage modulus as a function of temperature; Bis-EMA based systems.
- Figure 22:** Tangent delta curves as a function of temperature; Bis-EMA based systems.

## LIST OF TABLES

- Table 1:** Correlation between molecular weight, concentration of double bonds, viscosity and glass transition temperature of selected dimethacrylate monomers.
- Table 2:** Overview of the materials used (name, abbreviation, molecular mass, specific gravity and supplier).
- Table 3:** Summary of the light-cured resin systems characterized by DPC, FTIR and TGA.
- Table 4:** Summary of heat-cured resin systems characterized by DMA and FTIR.
- Table 5:** Mean and standard deviation values of maximum rate of polymerization ( $R_{p, \max}$ ), degree of conversion ( $P_{C=C}$ ) at  $R_{p, \max}$  and limiting degree of conversion ( $P_{C=C}$ ) as determined by DPC and FTIR; neat monomers.
- Table 6:** Mean and standard deviation values of temperature where thermal degradation start ( $T_0$ ), and the first ( $T_1$ ) and second ( $T_2$ ) maximum of thermal decomposition and residual mass at 600 °C; neat monomers.
- Table 7:** Mean and standard deviation values of maximum rate of polymerization ( $R_{p, \max}$ ), degree of conversion ( $P_{C=C}$ ) at  $R_{p, \max}$  and limiting degree of conversion ( $P_{C=C}$ ) as determined by DPC and FTIR; Bis-GMA/TEGDMA and Bis-EMA/TEGDMA copolymers.
- Table 8:** Mean and standard deviation values of temperature where thermal degradation start ( $T_0$ ), and the first ( $T_1$ ) and second ( $T_2$ ) maximum of thermal decomposition and residual mass at 600 °C; Bis-GMA/TEGDMA and Bis-EMA/TEGDMA copolymers.
- Table 9:** Mean and standard deviation values of the storage modulus at 40 °C ( $E'$ ) and at the point of glass transition ( $E'_{\text{rubbery}}$ ), glass transition temperature ( $T_g$ ) and limiting degree of double bonds conversion ( $P_{C=C}$ ) as determined by FTIR; neat monomers.
- Table 10:** Mean and standard deviation values of the storage modulus at 40 °C ( $E'$ ) and at the point of glass transition ( $E'_{\text{rubbery}}$ ), glass transition temperature ( $T_g$ ) and limiting degree of double bonds conversion ( $P_{C=C}$ ) as determined by FTIR; Bis-GMA/TEGDMA and Bis-EMA/TEGDMA copolymers.

## LIST OF ABBREVIATIONS

### Chemicals

<b>BD</b>	2,3-butanedione
<b>Bis-EMA</b>	Bisphenol A ethoxylate dimethacrylate
<b>Bis-GMA</b>	Bisphenol A glycidyl methacrylate
<b>CQ</b>	Camphorquinone; 2,3-bornanedione
<b>CQ (S)</b>	CQ excited singlet state
<b>CQ (T)</b>	CQ excited triplet state
<b>DEGDMA</b>	Diethylene glycol dimethacrylate
<b>DMAEMA</b>	(2-dimethylaminoethyl) methacrylate
<b>EDMAB</b>	Ethyl-4-dimethylamino benzoate
<b>PEGDMA</b>	Polyethylene glycol dimethacrylate
<b>PMMA</b>	Poly (methyl methacrylate)
<b>PPD</b>	1-phenyl-1,2-propanedione
<b>UDMA</b>	Urethane dimethacrylate
<b>TEGDMA</b>	Triethylene glycol dimethacrylate

### Experimental methods, others

<b>AFM</b>	Atomic Force Microscopy
<b>ATR</b>	Attenuated Total Reflection (mode of FTIR)
<b>DC</b>	Degree of double bond conversion
<b>DEA</b>	Dielectric Analysis
<b>DMA</b>	Dynamic Mechanical Analysis
<b>DSC</b>	Differential Scanning Calorimetry
<b>DPC</b>	Differential Photo Calorimetry
<b>EPR</b>	Electron Paramagnetic Resonance spectroscopy
<b>FTIR</b>	Fourier Transform Infra-Red Spectroscopy
<b>LCU</b>	Light Curing Unit
<b>LED</b>	Light Emitting Diode
<b>NMR</b>	Nuclear Magnetic Resonance spectroscopy
<b>PAC</b>	Plasma Arc
<b>PALS</b>	Positron Annihilation Lifetime Spectroscopy
<b>QTH</b>	Quartz Tungsten Halogen
<b>SEM</b>	Scanning Electron Microscopy
<b>TGA</b>	Thermo-Gravimetric Analysis

## Equations

$A$	Pre-exponential factor
$[A]$	Concentration of amine photo-reductant
$\beta$	Fraction of excited state complex forming free radicals
$[C_s]$	Concentration of photo-initiator
$[CQ_T^*]$	Concentration of CQ triplet state
$E'$	Storage modulus
$E''$	Loss modulus
$E^*$	Complex modulus
$E_a$	Activation energy
$\varepsilon$	Molar absorptivity of the photo-initiator
$h$	Heat flow
$\Delta H$	Enthalpy of reaction
$I_a$	Absorbed light intensity
$I_0$	Incident light intensity per unit area
$[M]$	Concentration of double bonds or monomer concentration
$[M^*]$	Concentration of all chain radicals
$N$	Number of measurements
$k$	Rate constant of the reaction
$k_a$	Rate constant for the exciplex formation
$k_p$	Propagation reaction kinetic constant
$k_t$	Termination reaction kinetic constant
$P_{C=C}$	Double bond conversion
$R$	Reaction-diffusion proportionality constant
$R$	Universal gas constant
$R_i$	Rate of initiation
$R_p$	Rate of propagation
$R_{p, \max}$	Maximal polymerization rate on the time/conversion scale
$R_r$	Rate of production of primary free radicals from photosensitizer
$R_t$	Rate of termination
$\rho$	Density of the resin system
$T$	Absolute temperature
$T_g$	Glass transition temperature
$\phi$	Quantum yield for photo-initiation

## AUTHOR'S CV

### *Personal Information*

Name	Ing. Bc. Zdeněk Bystřický
E-mail	bystricky@dentapreg.com
Date of birth	13/01/1988

### *Education*

Dates	2012–2019
Degree and Discipline	Doctoral; Macromolecular Chemistry
Organization	Brno University of Technology, Faculty of Chemistry

Dates	2010–2012
Degree and Discipline	Master's; Chemistry, Technology and Properties of Materials
Organization	Brno University of Technology, Faculty of Chemistry

Dates	2010–2011
Discipline	Materials Engineering, Winter Semestral Traineeship
Organization	Instituto Superior Técnico, Lisbon, Portugal

Dates	2009–2013
Degree and Discipline	Bachelor's; Microbiology
Organization	Masaryk University, Faculty of Science

Dates	2007–2010
Degree and Discipline	Bachelor's; Chemistry, Technology and Properties of Materials
Organization	Brno University of Technology, Faculty of Chemistry

### *Employment*

Dates	2014–2015
Position	Scientific Employee, Ph.D. student
Organization	Central European Institute of Technology – CEITEC (Materis project)

Dates	2015–2019
Position	Manager of Research and Innovations
Organization	Advanced Dental Materials – ADM, a.s.

## ***Publications***

BYSTRICKÝ, Z., Z. ŠEDIVÝ, O. SLAVÍK a T. SLAVÍČEK. *Dentální materiál na bázi částicového kompozitu, Patent 2018. CZ307577B6. Uděleno 07.11.2018.*

BYSTRICKÝ, Z. and JANČÁŘ, J. Morphogenesis of Photo-Polymerized Dimethacrylate Networks, Kinetics of Curing and Viscoelastic Parameters. *Materials Science Forum*, 2016, č. 851, s. 207-214. ISSN: 0255-5476.

VACEK, L., BYSTRICKÝ, Z., RŮŽIČKA, F., a JANČÁŘ, J. Adherence a růst biofilmu *Streptococcus mutans* na dentálních restorativních materiálech. In XXV. Tomáškovy dny mladých mikrobiologů. 2016. ISBN 978-80-210-8255-7.

BYSTRICKÝ, Z., VACEK, L., RŮŽIČKA, F., and JANČÁŘ, J. *Adherence and Growth of Cariogenic Biofilms on Dental Dimethacrylate- Based Resin Substrates*. Brno: 2015. s. 60-60.

BYSTRICKÝ, Z. and JANČÁŘ, J. *Morphogenesis of Photo-Polymerized Dimethacrylate Networks, Network Formation Kinetics and Viscoelastic Parameters*. Chemistry and Life 2015, Book of Abstracts. 1. Brno: Brno University of Technology, Faculty of Chemistry, Purkynova 464/118, CZ- 612 00 Brno, 2015. s. 179-179. ISBN: 978-80-214-5228- 2.

BYSTRICKÝ, Z. and JANČÁŘ, J. *Morphogenesis and viscoelastic properties of dental dimethacrylate networks*. Book of Abstracts, CEITEC Annual Conference "Frontiers in Material and Life Sciences". Brno, Czech Republic: Masaryk University, 2014. ISBN: 978-80-210-7159.

BYSTRICKÝ, Z. and JANČÁŘ, J. Network Formation by Dimethacrylate Based Dental Resins, Evolution of the Structure and Viscoelastic Parameters. In *Studentská odborná konference Chemie je život 2014*. Brno, Czech Republic: Vysoké učení technické v Brně, Fakulta chemická, Purkyňova 464/118, 612 00 Brno, 2014. s. 201-210. ISBN: 978-80-214-5078- 3.

BYSTRICKÝ, Z. a POLÁČEK, P. Pevnost adhezního spoje mezi vláknovým a částicovým kompozitem. In *Víceúrovňový design pokrokových materiálů, sborník doktorské konference 2011*. Brno: Ústav fyziky materiálů AV ČR, v. v. i., 2011. s. 73-80. ISBN: 978-80-87434-04- 8.